Tianlai cylinder array system and analysis

Jixia Li

NAOC, China

Outline

- Introduction
- Tianlai cylinder system
- Performance analysis
- Reflection analysis
- Summary

Tianlai project: antenna array

- Antenna area
  - Dish array and cylinder array.
  - Comparison of two types of antennas in HI sky survey.
  - Calibrator Noise Source (CNS) , periodic broadcast

Tianlai project: naming convention

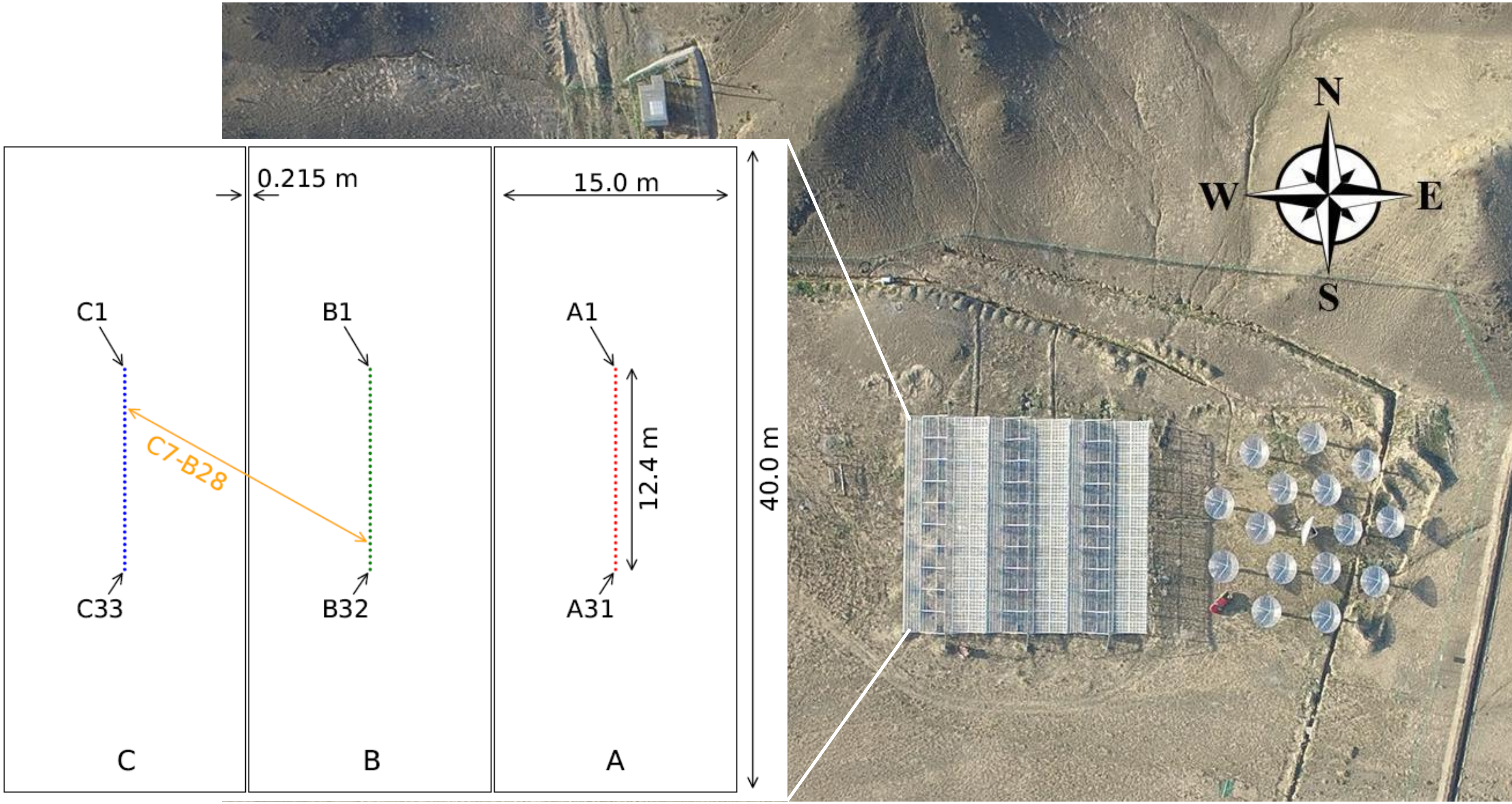

- Antenna area
  - Dish array and cylinder array.
  - Comparison of two types of antennas in HI sky survey.

Tianlai project: location

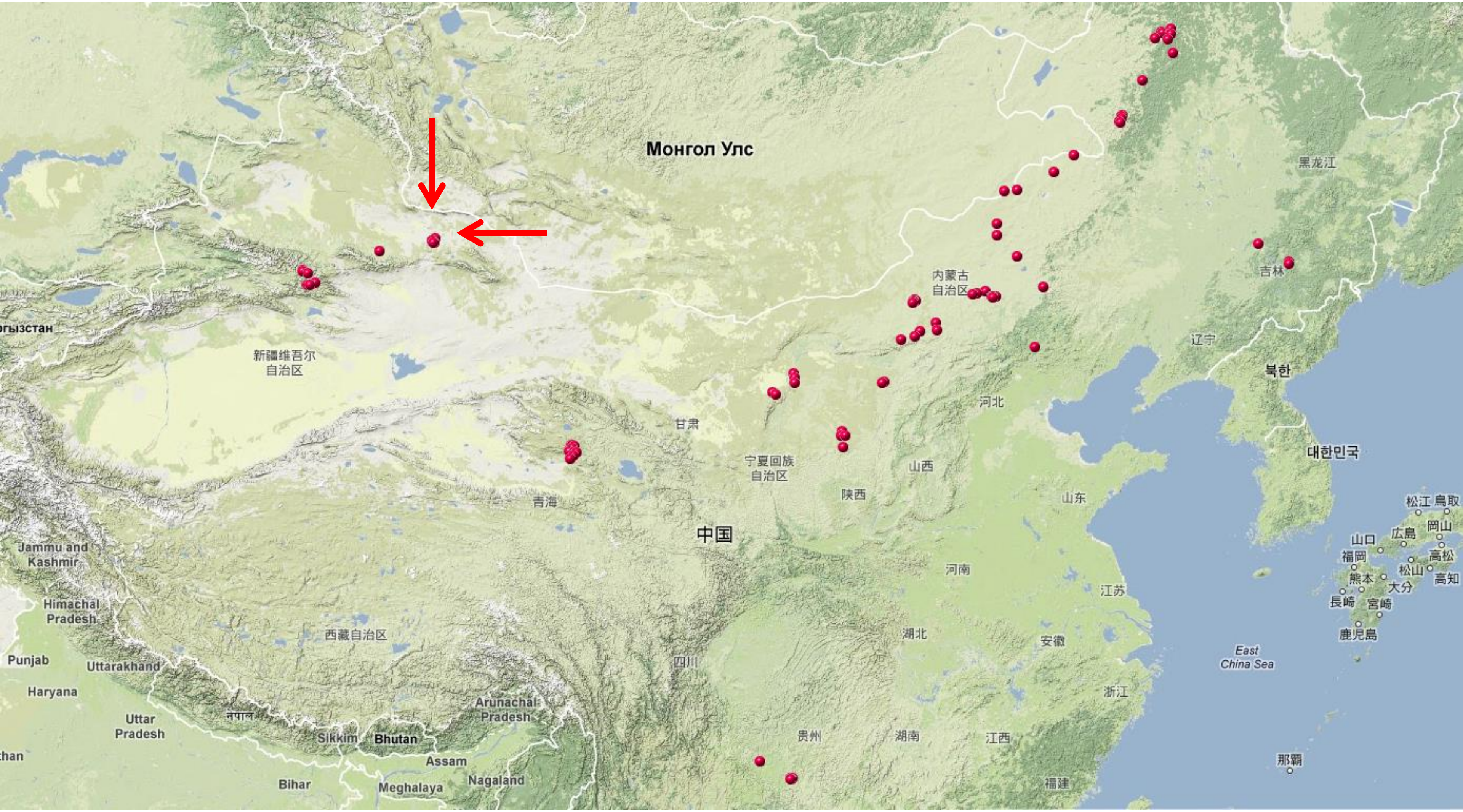

- HongLiuXia Observatory
  - Dahongliuxia, Balikun, Hami, Xinjiang (E 91.806867 deg; N 44.152683 deg)
  - Very radio-quiet.

Tianlai project: radio environment

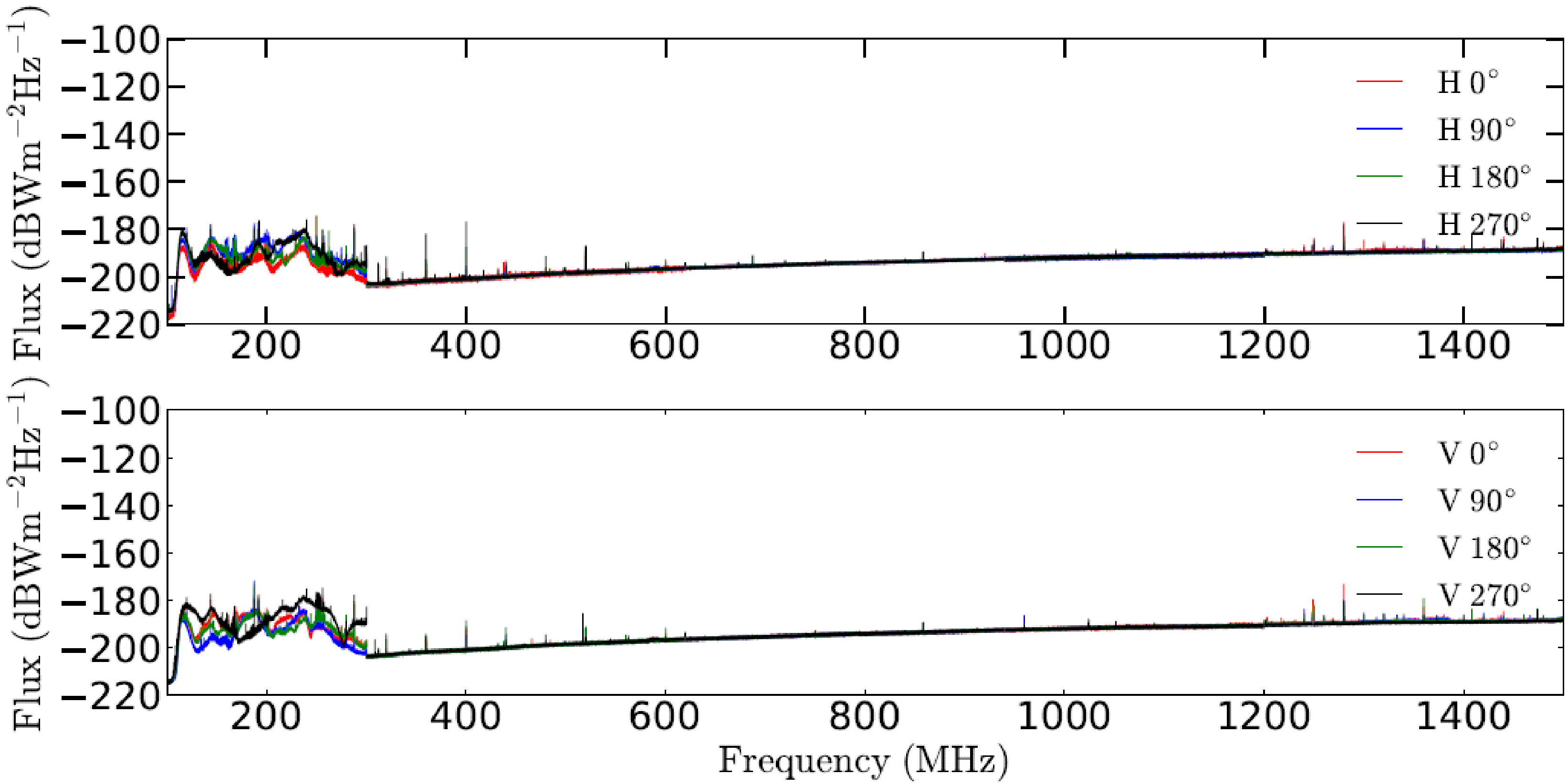

- Current frequency range
  - 700-800 MHz, almost none.
  - RFI removed later.
- L band RFI source
  - Navigation, digital broadcasting satellite, communication satellite.

Tianlai project: optic cable

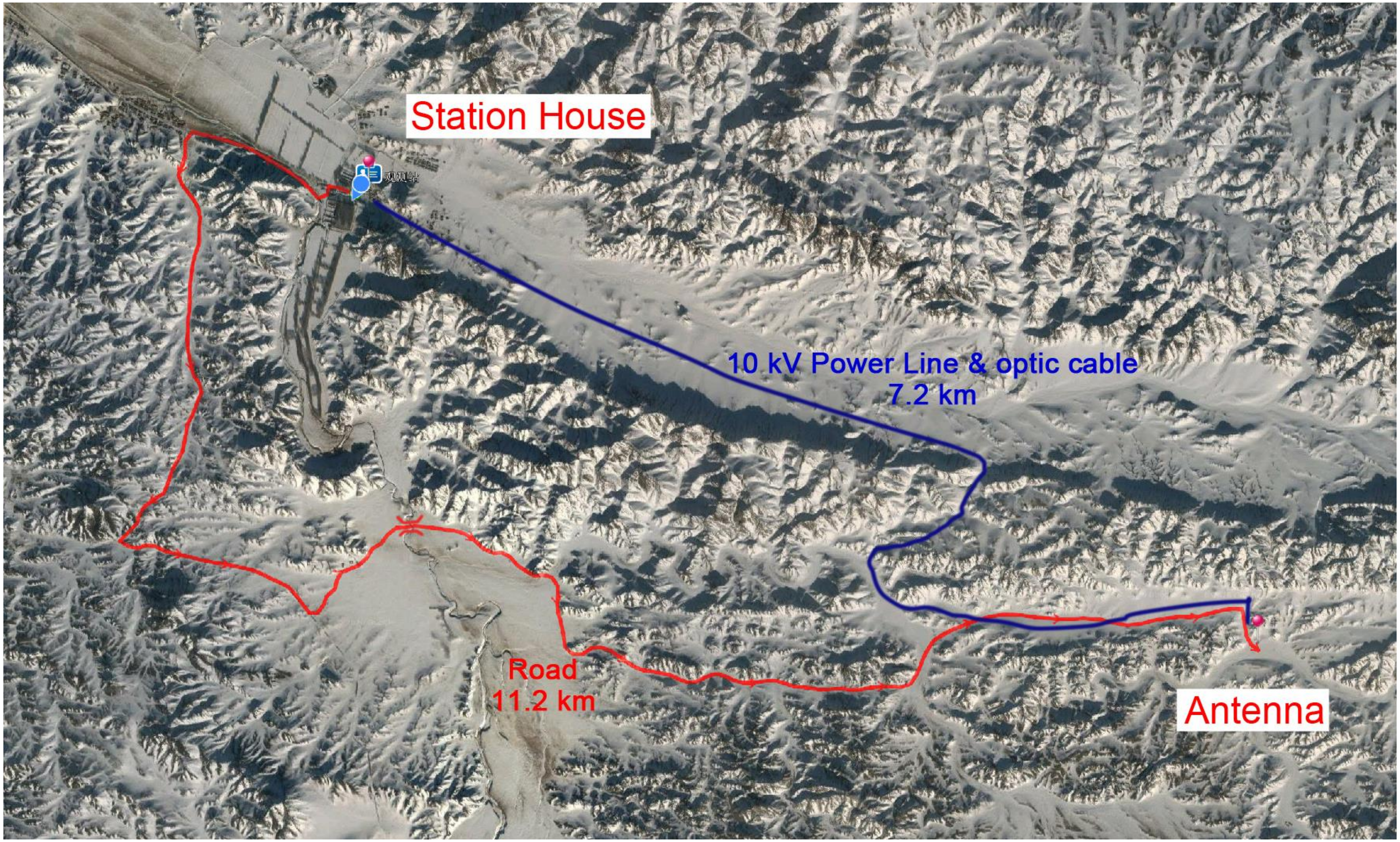

- Station house area
  - 6 km in distance, 11.2 km by road (30 mins' drive).
  - RFI of digital devices are avoided.

Tianlai project: schematic

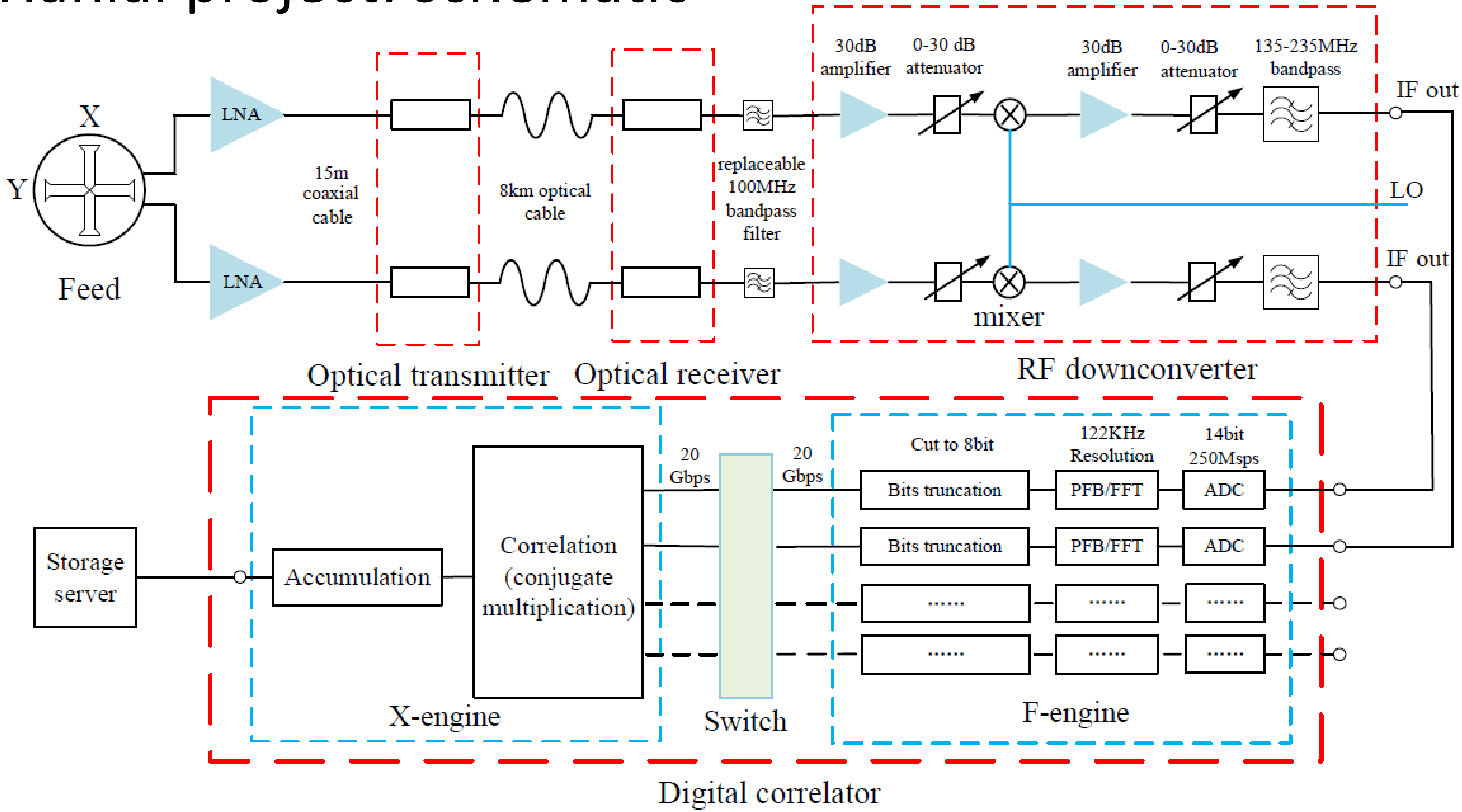

- Schematic of analog and digital systems.
  - 700-800 MHz
  - 250 Msps, 2048-point FFT, 122 kHz resolution
  - 3.995 sec integration time

Tianlai project: data and process

- Data amount: ~400 TB (>100 days)
- Data transport by hard disks
  - Tianlai site → Beijing (Preliminary analysis) → Tianhe (full scale analysis)
- Data process (tlpipe*)

RFI flagging
↓
Absolute calibration
↓
Relative calibration
↓
Quality check
↓
LST time binning
↓
Map-making

Data Process

Data set	Lengths (d)	Malfunction channels
2016/09/27 20:15:37	5	A18Y, A28, B19, C7Y, C9X, C14X, C16, C29Y
2016/10/11 00:49:48	5	A18Y, A28, B19, C7Y, C9X, C14X, C16, C29Y
2016/12/31 20:51:54	17	Many
2017/02/13 19:23:07	5	A18Y, A24Y, B6Y, B26Y, C15X, C7Y
2017/02/24 19:31:07	9	A18Y, A24Y, B6Y, B26Y, C15X, C7Y, C18-C33
2017/08/21 21:26:39	3	A26X, B21X, C3X, C16, A17-A24, C26-C33
2017/09/03 14:32:17	9	A26X, B21X, C3X, C16, A17-A24, C26-C33
2017/09/22 01:33:18	7	A26X, B21X, C3X, C16, A17-A24, C26-C33
2017/09/29 21:42:59	13	A26X, B21X, C3X, C16, A17-A24, C26-C33
2017/12/09 19:21:54	10	A18Y, A24Y, A26X, B26Y, B31X
2017/12/20 19:22:02	4	A18Y, A24Y, A26X, B26Y, B31X
2018/01/21 00:05:35	14	A18Y, A24Y, A26X, B26Y, B31X, C28Y
2018/03/22 18:07:58	9	A18Y, A24Y, A26X, B26Y, B31X, C28Y
2018/03/31 17:08:12	4	A18Y, A24Y, A26X, B26Y, B31X, C28Y
Total	114 d	

Observation data list

* Shifan Zuo, Jixia Li et al. 2020 (submitted) https://tlpipe.readthedocs.io

Hardware tests: feed S11 & LNA

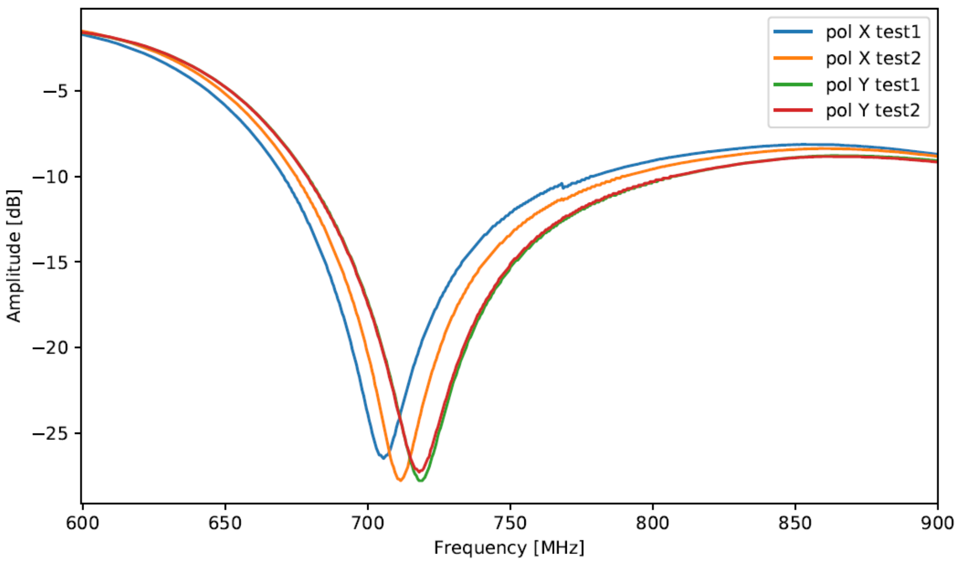

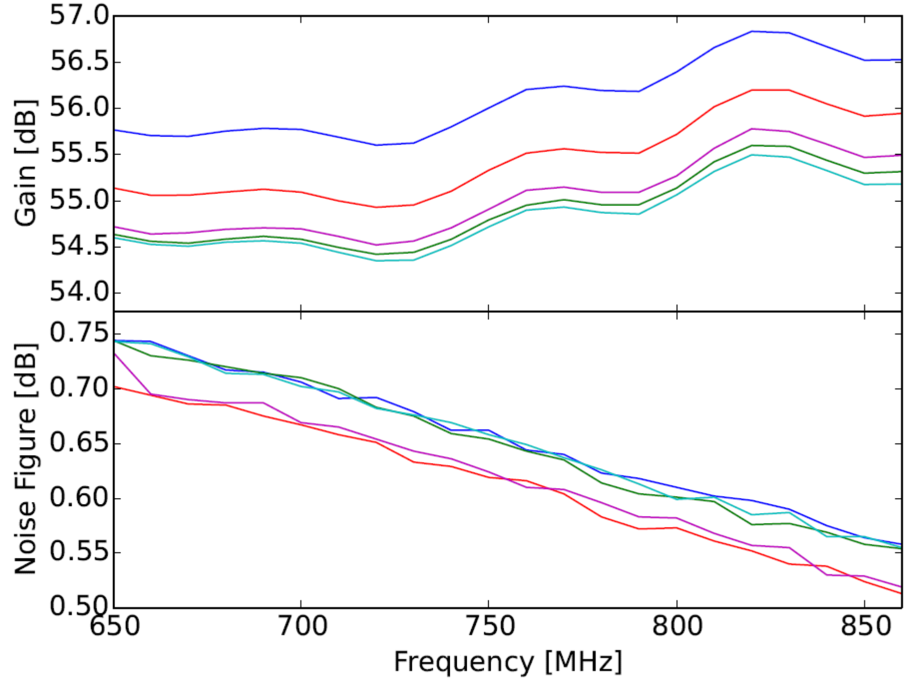

LNA gain and NF

Feed reflection

- Test in open space, may have reflections from surround.
- 700-730 MHz
  $< -15\mathrm{dB}$ very low reflection.
- 730-800 MHz
  $< -9\mathrm{dB}$.

Gain ≈ 55 dB

NF ≈ 0.65 dB, 0.1 dB variation

Noise temperature

$$T = \left(10^{\frac{\mathrm{NF}}{10}-1}\right) \times T_0$$

$T_{\mathrm{LNA}} \approx 47$ K @ 290 K.

Hardware tests: linearity of LNA and mixer

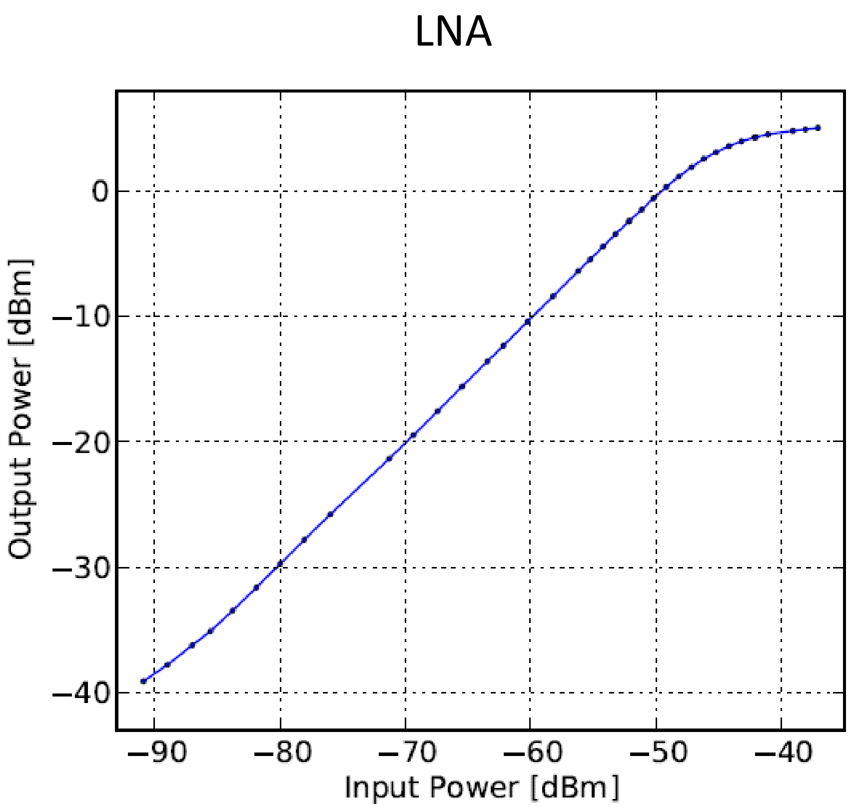

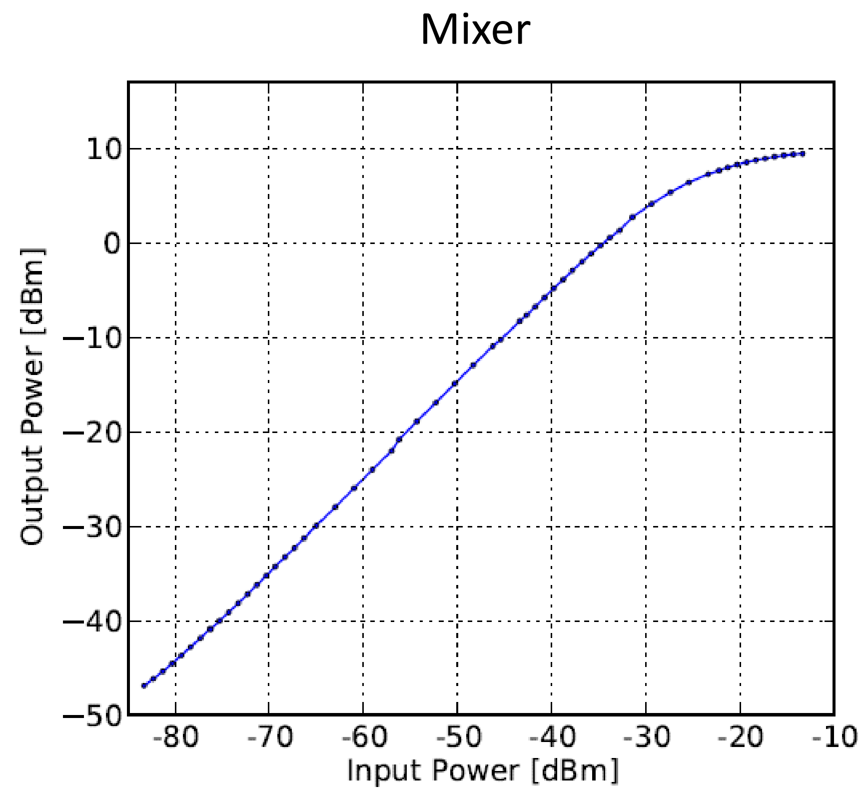

- Input wideband noise of different levels.
- Measure the total channel power in band.
- Discontinuity caused by attenuations and pre-amplifier of spectrum.
- Good linearity.

Hardware tests: linearity of ADC

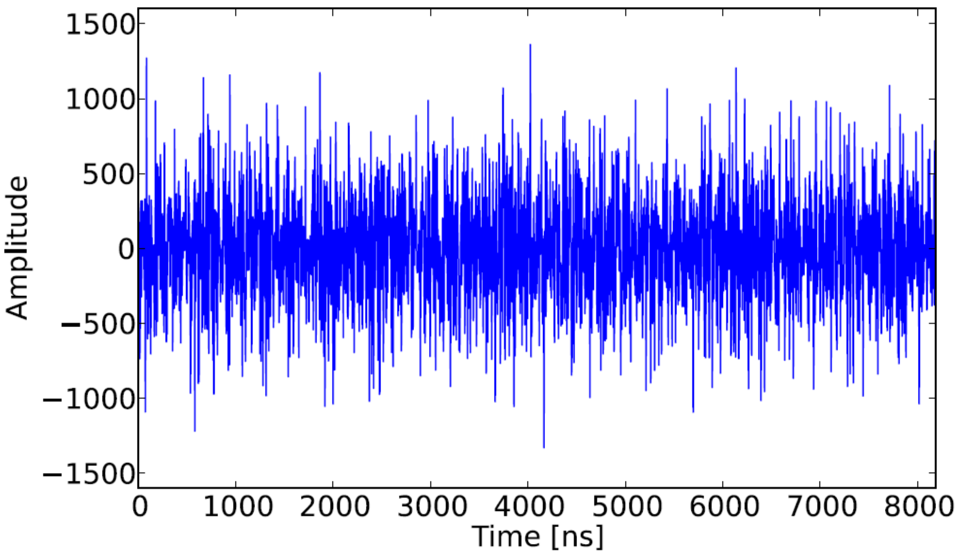

ADC time stream samples

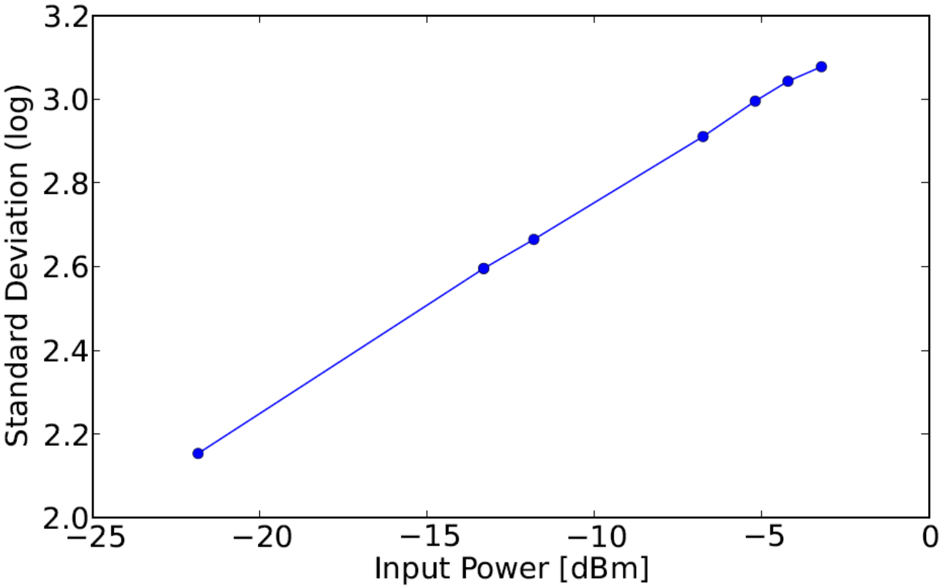

STD vs input power

- Input wideband noise of different levels.
- Take down ADC time stream samples.
- Calculate standard deviation of the raw samples.
- Current @ -13 dBm / 125 MHz at night when no source
  - 30 dB + 30 dB electric control attenuator inside mixer
  - 5 % of total AD range (14 bits).

Hardware tests: linearity

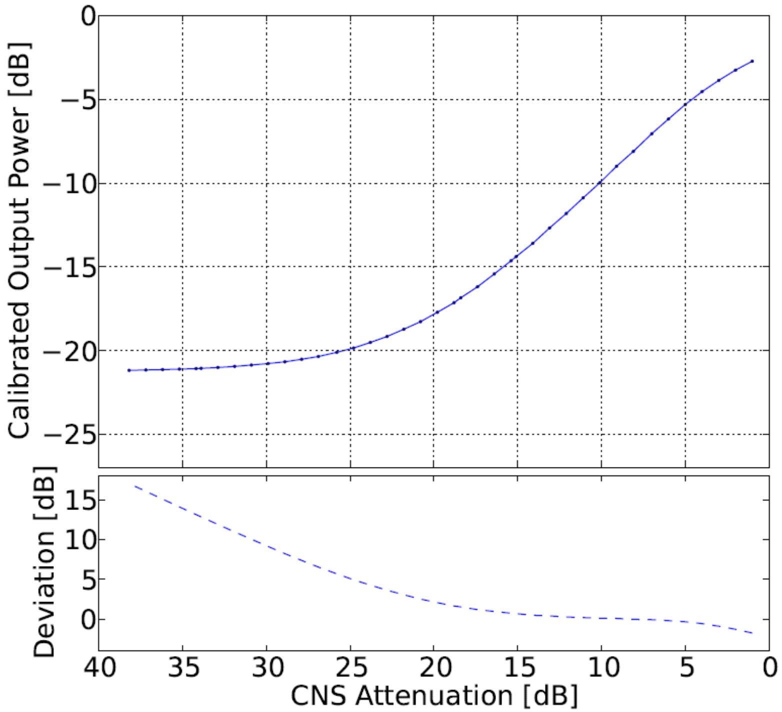

Auto-correlation

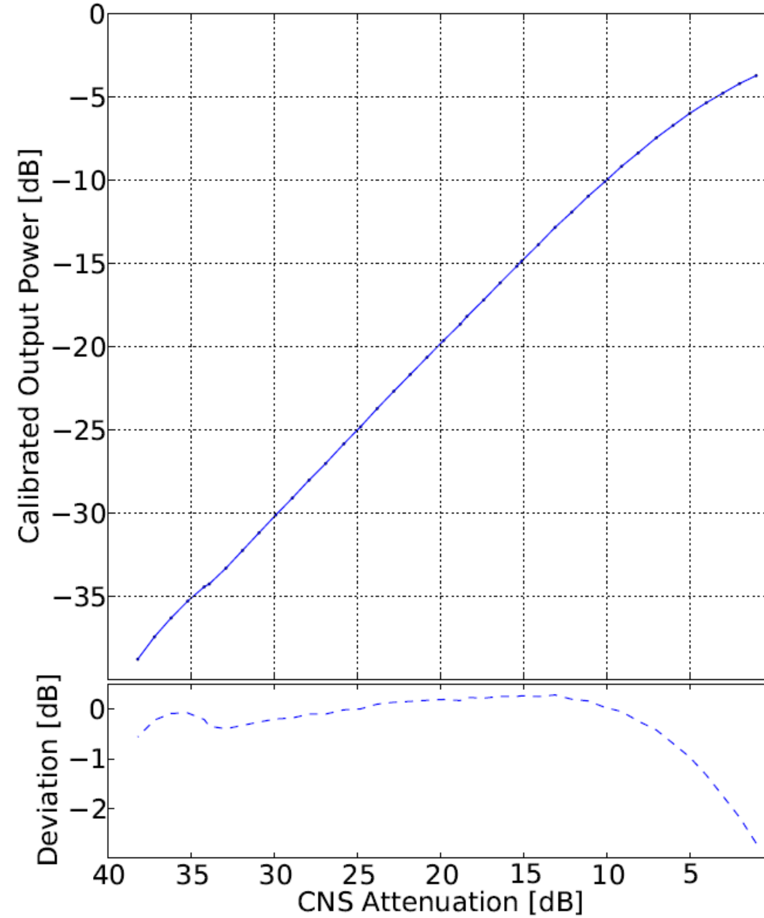

Cross-correlation

- Input Calibrator Noise Source (CNS) of different levels.
  - Levels achieved with different attenuators.
- Calculate the auto- and cross-correlation amplitude.
- Auto-correlation
  - ~ 10 dB range; P1dB point≈ -3 dB; ground level: noise and sky signal.
- Cross-correlation
  - > 35 dB range.

Hardware tests: phase variation of optic cable

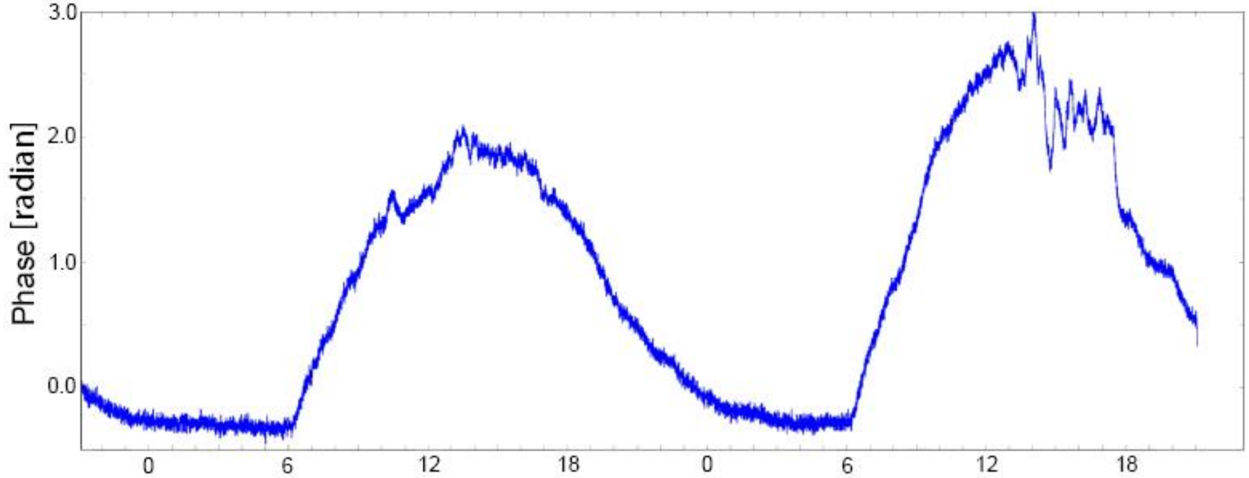

8 km optic cable
phase variation
of cross-correlation

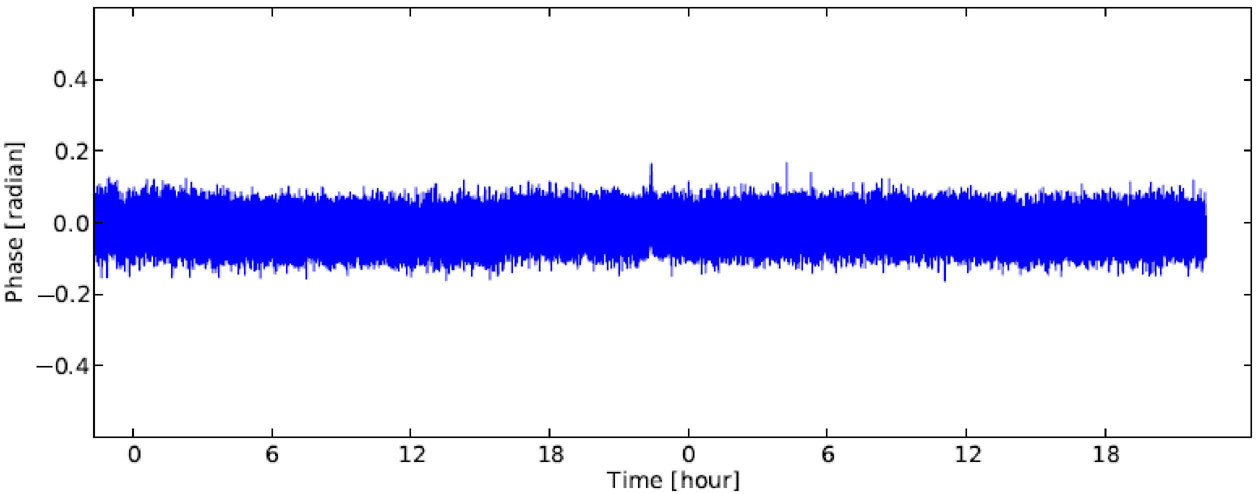

Phase variation of
analog devices
(2-m optic fiber)

- 50 Om shared by power splitter; 2 days continuous observation.
- Instrumental phase variation mostly comes from optic cable part.
- Most of the signal chains: $\Delta\phi < 2\pi$
- Strongly related to temperature.

Visibility fringes: raw data

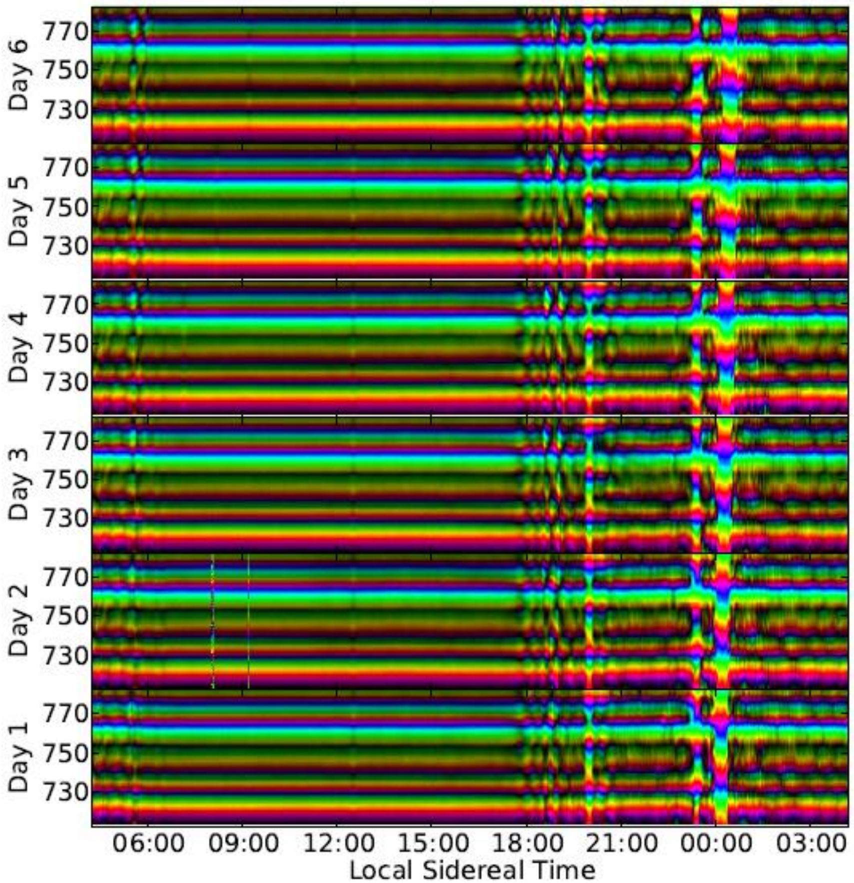

A3Y-A15Y

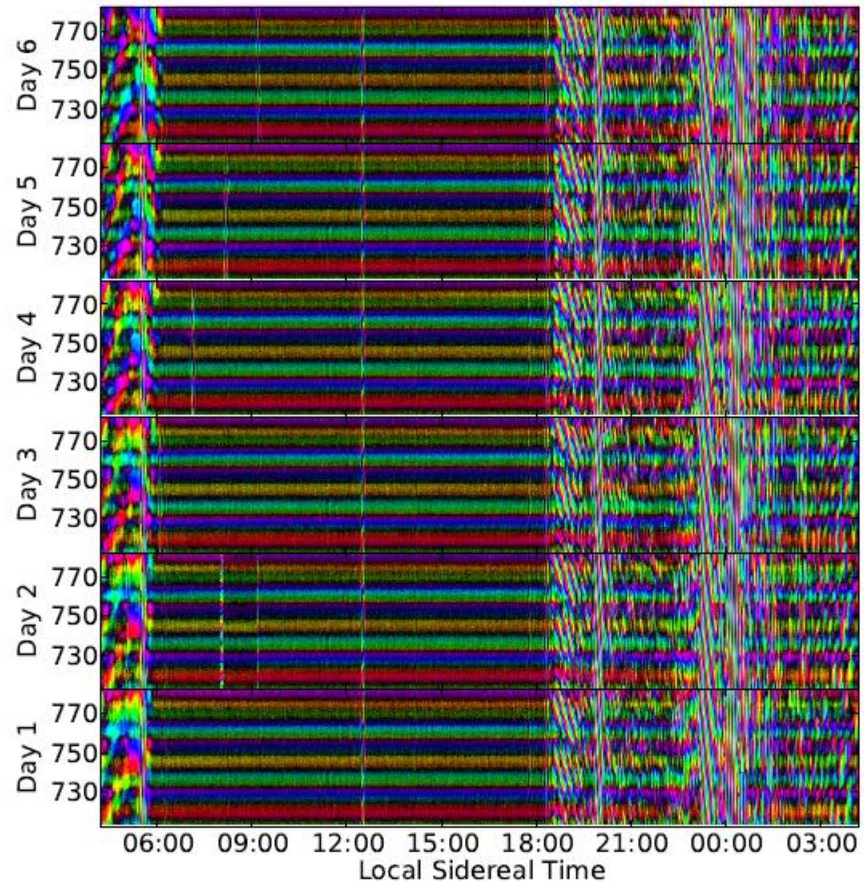

A3Y-B18Y

- 2018/03/22 data, 6 days' continuous observation.
- Rebinned to 488 kHz, 20-second integration time.
- Short baselines→stronger cross couplings.
- Sources: Moon, Virgo A, Sun, Dish reflections.

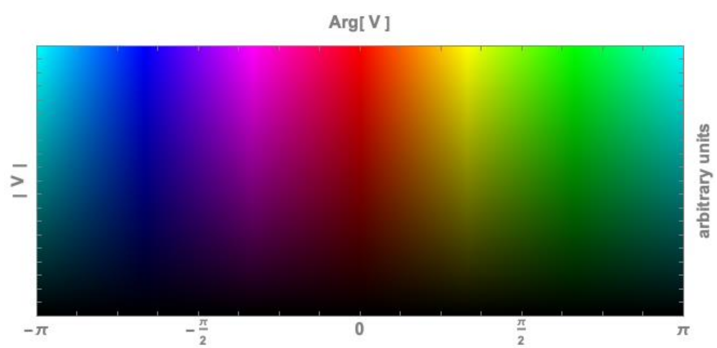

Visibility fringes: remove cross couplings

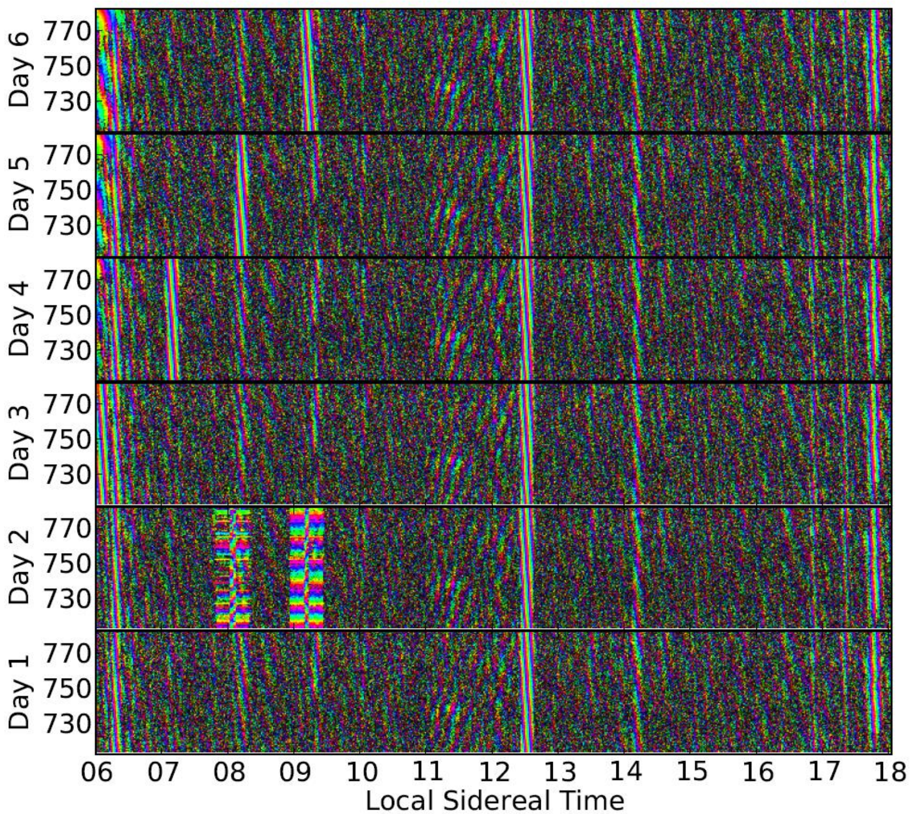

2018/03/22, A3Y-B18Y

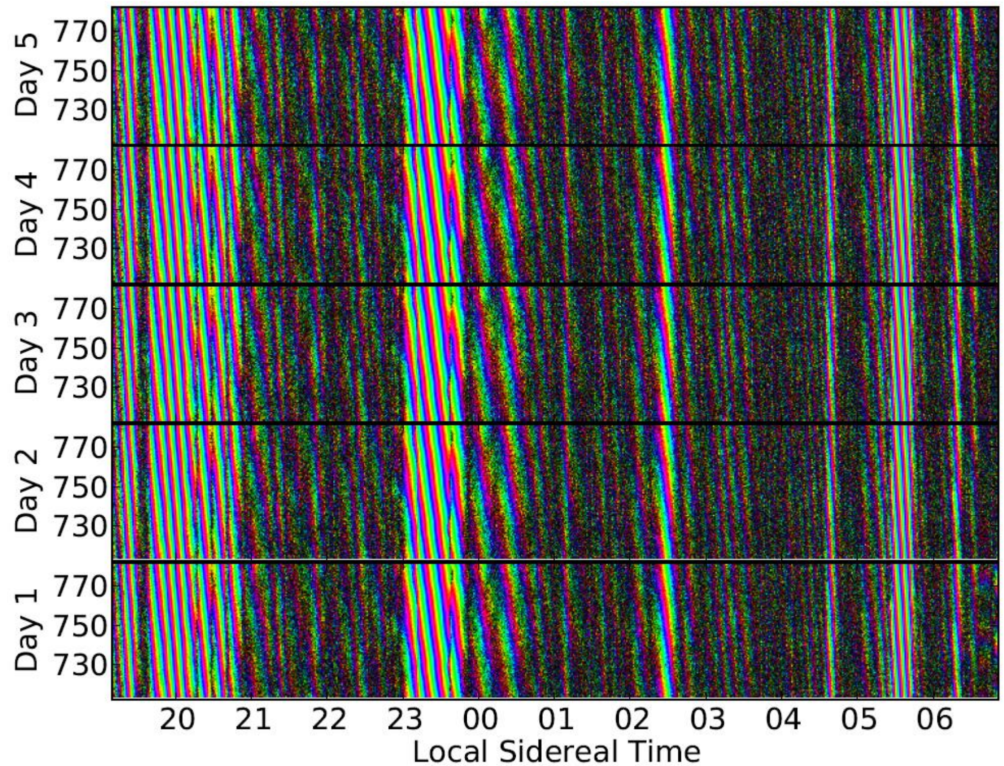

2016/09/27, A1Y-B2Y

- Only use night-time data.
- Darker sources are visible after cross-couplings removed by smoothed moving average.
- 2018/03/22: spring night. 2016/09/27: autumn night.
- Recognize sources for full sky.

Visible Sources

Source	RA	Zenith (deg)	Flux (Jy)		Source	RA	Zenith (deg)	Flux (Jy)
3C 010	00:25	20.0	62		3C 295	14:11	8.1	37
3C 058	02:05	20.7	34		Hercules A	16:51	39.2	88
IC 1805	02:32	17.4	--		3C 353	17:20	45.1	88
3C 084	03:20	2.7	22		GC	17:45	73.0	-
3C 123	04:37	14.5	76		3C 380	18:29	4.6	23
M 1	05:34	22.15	-		3C 392	18:56	42.8	242
M 42	05:35	49.5	-		3C 400	19:23	30.0	673
IC 443	06:16	21.6	190		Cyg A	19:59	3.4	2980
3C 196	08:13	4.1	23		Cyg X	20:28	41.2	-
Hydra A	09:18	56.2	81		NRAO 650	21:12	8.3	48
M 87	12:30	31.8	353		3C 433	21:24	19.1	21
3C 286	13:31	13.6	19		Cas A	23:23	14.7	2861

- 2018/03/22 spring night + 2016/09/27 autumn night.
- Source information obtained from NASA/IPAC Extragalactic Database.
- Flux @ 750 MHz. Some are radio compounds.

Data analysis: beam simulation

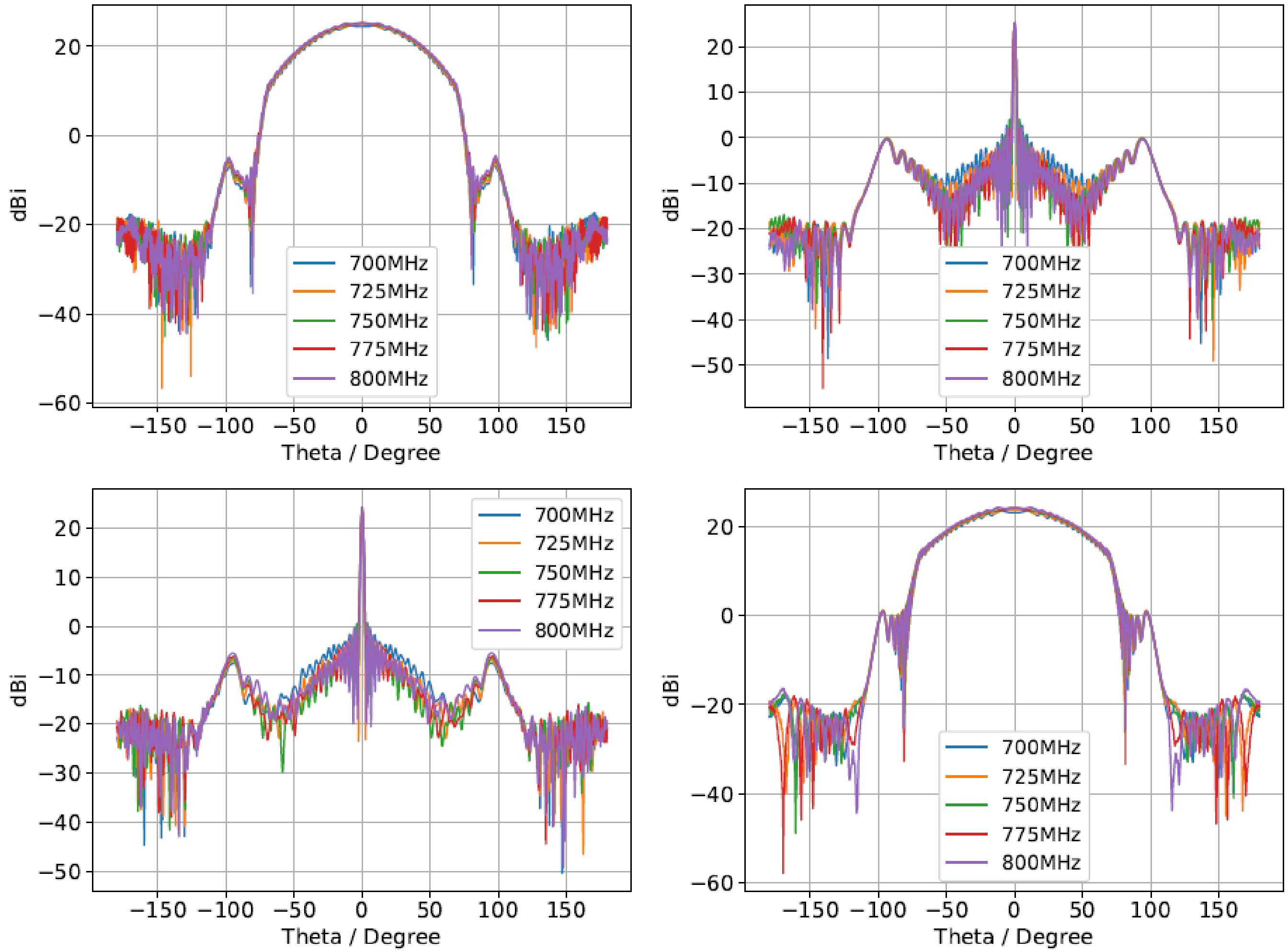

- Directivity along N-S and E-W direction for both E-plane and H-plane.

Data analysis: beam pointing – auto-correlation

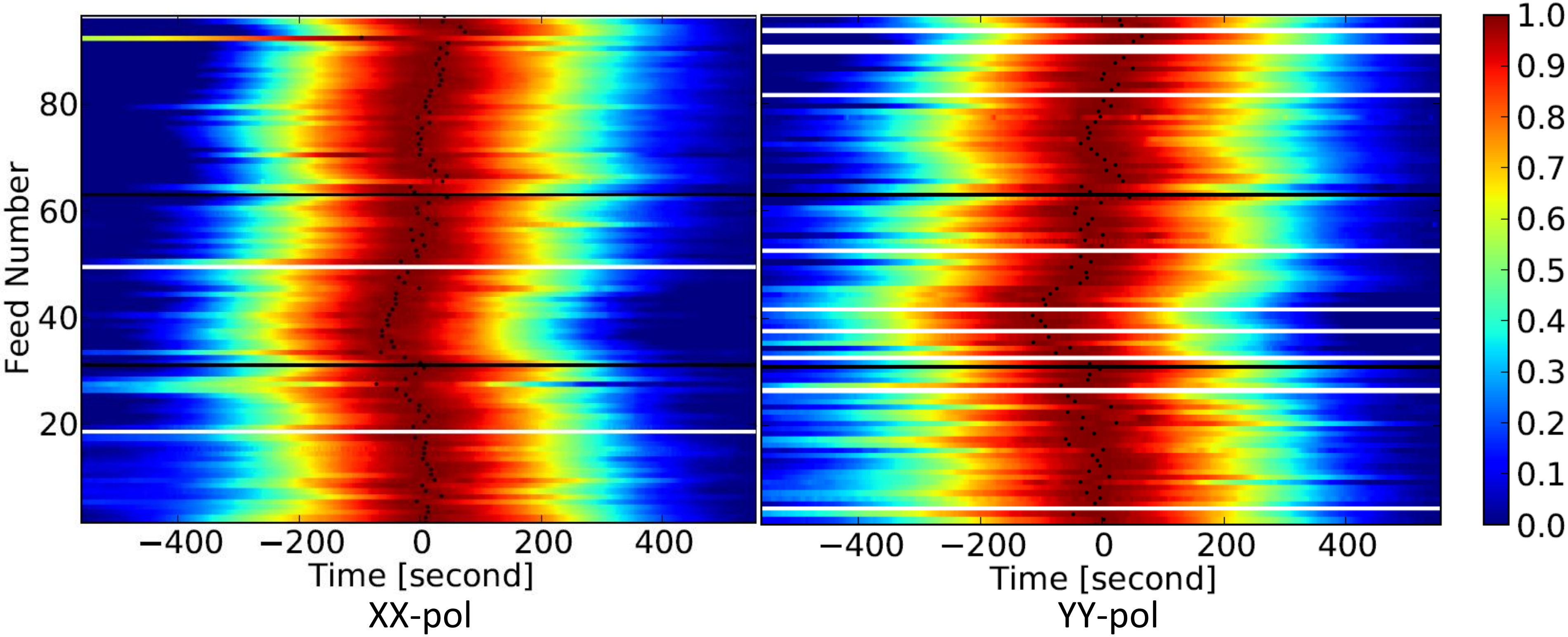

- Source: Cyg A
- Amplitude averaged over all frequency points.
- Amplitude vs time curve fitted by Gaussian; black points are peaks.
- $\sigma_\mathrm{X} = 31.1\ \mathrm{s} \rightarrow 0.099°$, $\sigma_\mathrm{Y} = 38.8\ \mathrm{s} \rightarrow 0.123°$
- Cyg A is near to Cyg X and Milky Way
  - A linear background is fitted and removed.
  - Confused emission removal introduces errors → cross-correlation is better.

Data analysis: beam pointing – cross-correlation

$\mathbf{A_B}$	$\mathbf{A_C}$
$\mathbf{B_C}$	$\mathbf{B_A}$
$\mathbf{C_A}$	$\mathbf{C_B}$

$\mathrm{A_B}$:

A1-B1
A1-B2
⋮
A1-B32

A2-B1
A2-B2
⋮
A2-B32

⋮
⋮
A31-B32

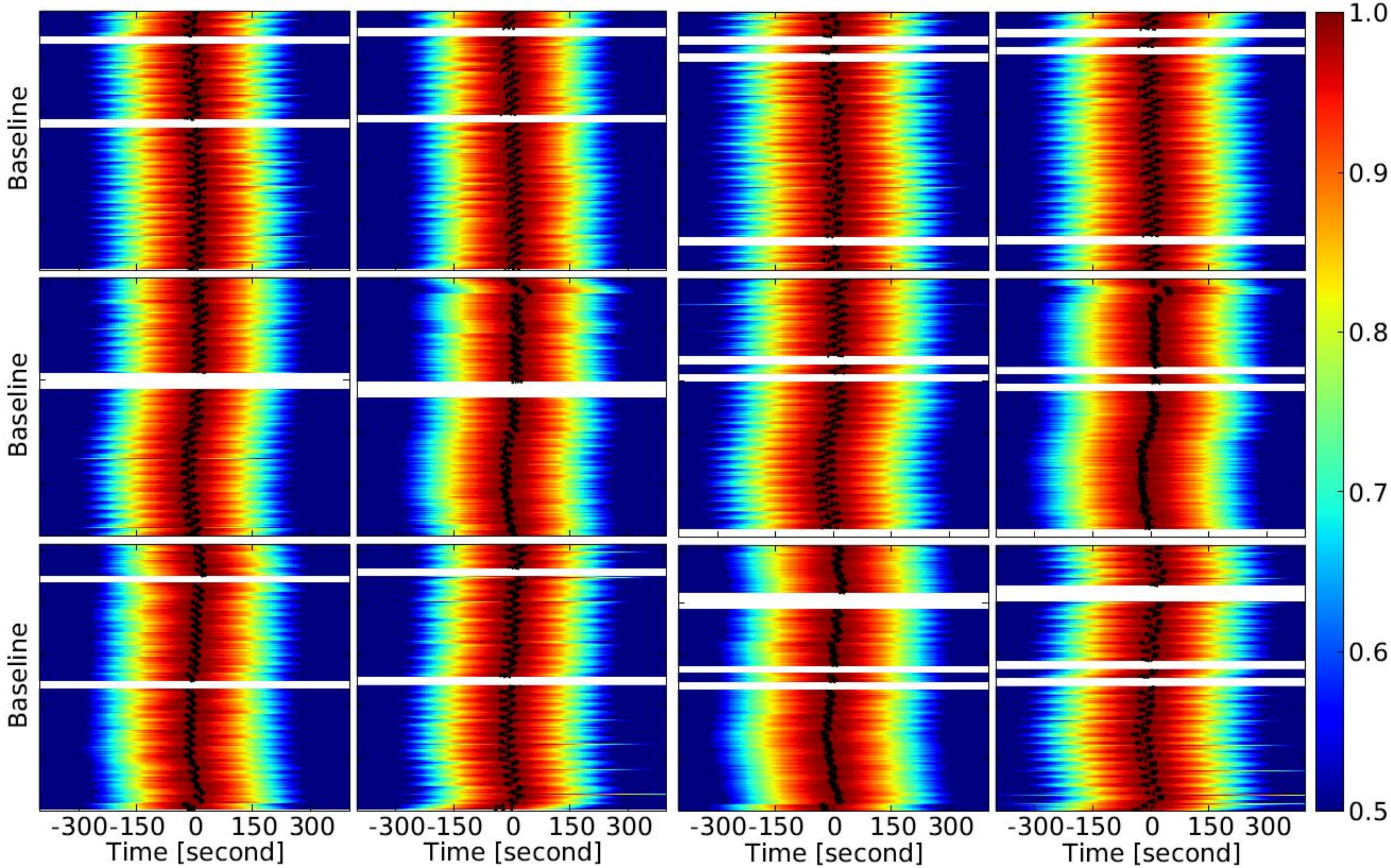

- Cross-correlation amplitudes vs time. (Only use correlations spanning 2 cylinders.)
- $\mathrm{A_B}$ and $\mathrm{A_C}$ are similar. Two polarizations are similar.
- General distribution reflects the beam pointing → Calculate average curve.

Data analysis: beam pointing – cross-correlation

- For feed Al and $\mathrm{B}m$, pointing are $\theta_{al} = a_l$ and $\phi_{bm} = b_m$.
- Cross-correlation beam pointing is $\gamma_{al-bm} = \frac{1}{2}(a_l + b_m)$.
- Setup many equations
  - Unknown pointing parameters: 96
  - Number of equations: 6142

$$
\begin{aligned}
a_l &= \frac{1}{M}\sum_{m=1}^{M}\theta_{l,m}^{\mathrm{AB}} + \frac{1}{N}\sum_{n=1}^{N}\phi_{l,n}^{\mathrm{AC}} - \frac{1}{MN}\sum_{m=1}^{M}\sum_{n=1}^{N}\gamma_{m,n}^{\mathrm{BC}} \\
b_m &= \frac{1}{N}\sum_{n=1}^{N}\theta_{m,n}^{\mathrm{BC}} + \frac{1}{L}\sum_{l=1}^{L}\phi_{m,l}^{\mathrm{BA}} - \frac{1}{NL}\sum_{n=1}^{N}\sum_{l=1}^{L}\gamma_{n,l}^{\mathrm{CA}} \\
c_n &= \frac{1}{L}\sum_{l=1}^{L}\theta_{n,l}^{\mathrm{CA}} + \frac{1}{M}\sum_{m=1}^{M}\phi_{n,m}^{\mathrm{CB}} - \frac{1}{LM}\sum_{l=1}^{L}\sum_{m=1}^{M}\gamma_{l,m}^{\mathrm{AB}}
\end{aligned}
$$

- Though number of equations >> unknown parameters, a hypothesis:
  - Average pointing error is zero, or at least very small.

Data analysis: beam pointing – cross-correlation

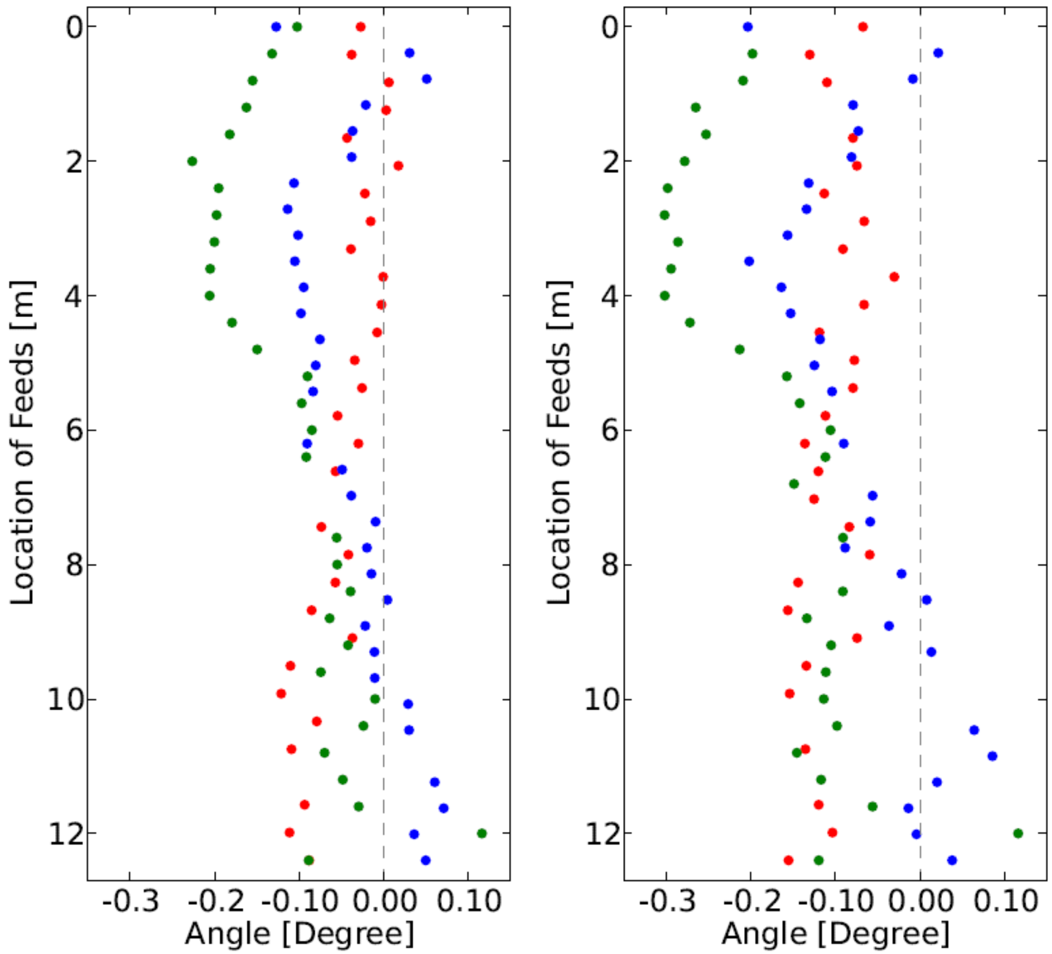

Red: Cylinder A
Green: Cylinder B
Blue: Cylinder C

Left: XX pol
Right: YY pol

- Two types of pointing errors
  - Feed supporters → tiny adjustment
  - Feed misalignment: $\sim 0.05°$ - a proper error for manual installation.
- Introduce errors on precision observations.

Data analysis: beam width – cross-correlation

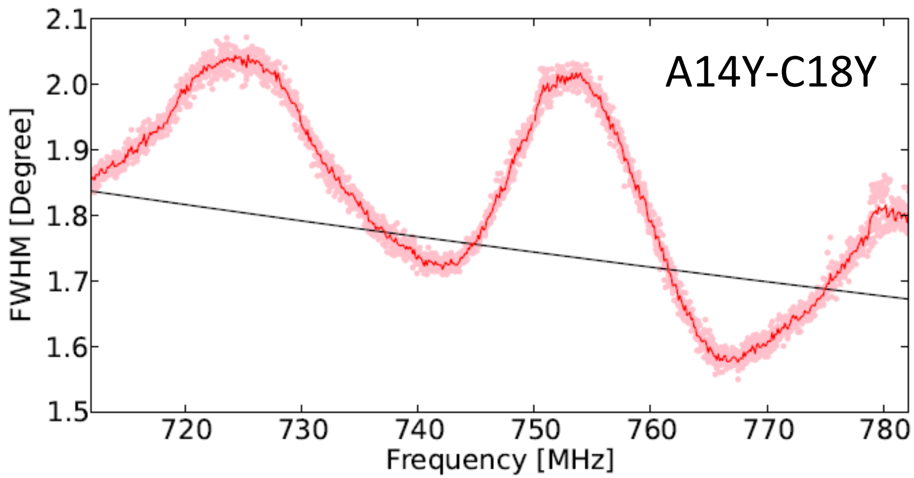

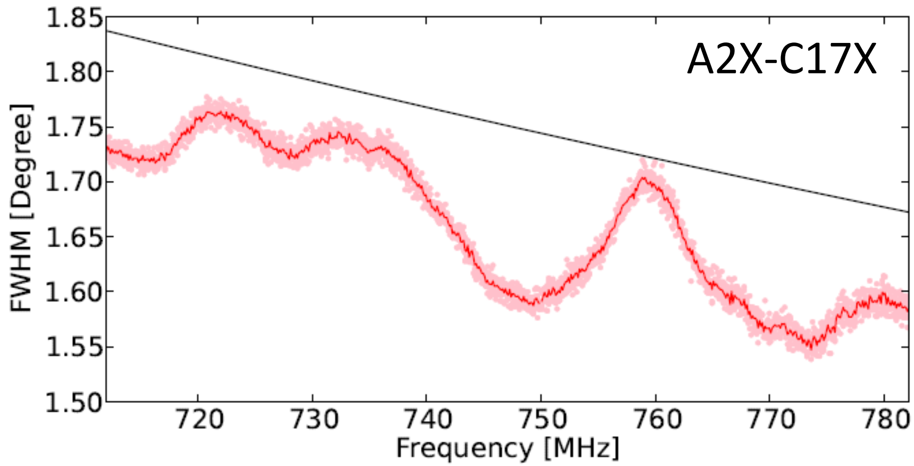

Diretivity

$$D = \frac{P_{\max}(\theta, \phi)}{P_{\mathrm{mean}}}$$

$$P_{\mathrm{mean}} = \frac{1}{4\pi}\int P(\theta,\phi)\mathrm{d}\Omega$$

$$D = \frac{4\pi}{\Omega_{\mathrm{A}}}$$

Effective area

$$A_{\mathrm{e}} = \frac{D\lambda^2}{4\pi}$$

$$D_{\mathrm{X}} = 25.2\mathrm{dBi}$$
$$D_{\mathrm{Y}} = 24.2\mathrm{dBi}$$
$$A_{\mathrm{e}}^{\mathrm{X}} = 4.22\mathrm{m}^2$$
$$A_{\mathrm{e}}^{\mathrm{Y}} = 3.35\mathrm{m}^2$$

- Pink dots: 7 days beam width fitted at each frequency. (2018/03/22 Cyg A)
- Red Curve: average over 7 days. Day-t-day variation $< 3\%$
- Wiggles indicate standing waves in antenna. Similar to CHIME (Newburgh et al. 2014)
- Diffraction-limited circular aperture ($1.028\lambda/0.9\mathrm{D}$)

Calibration: bandpass of Cyg A

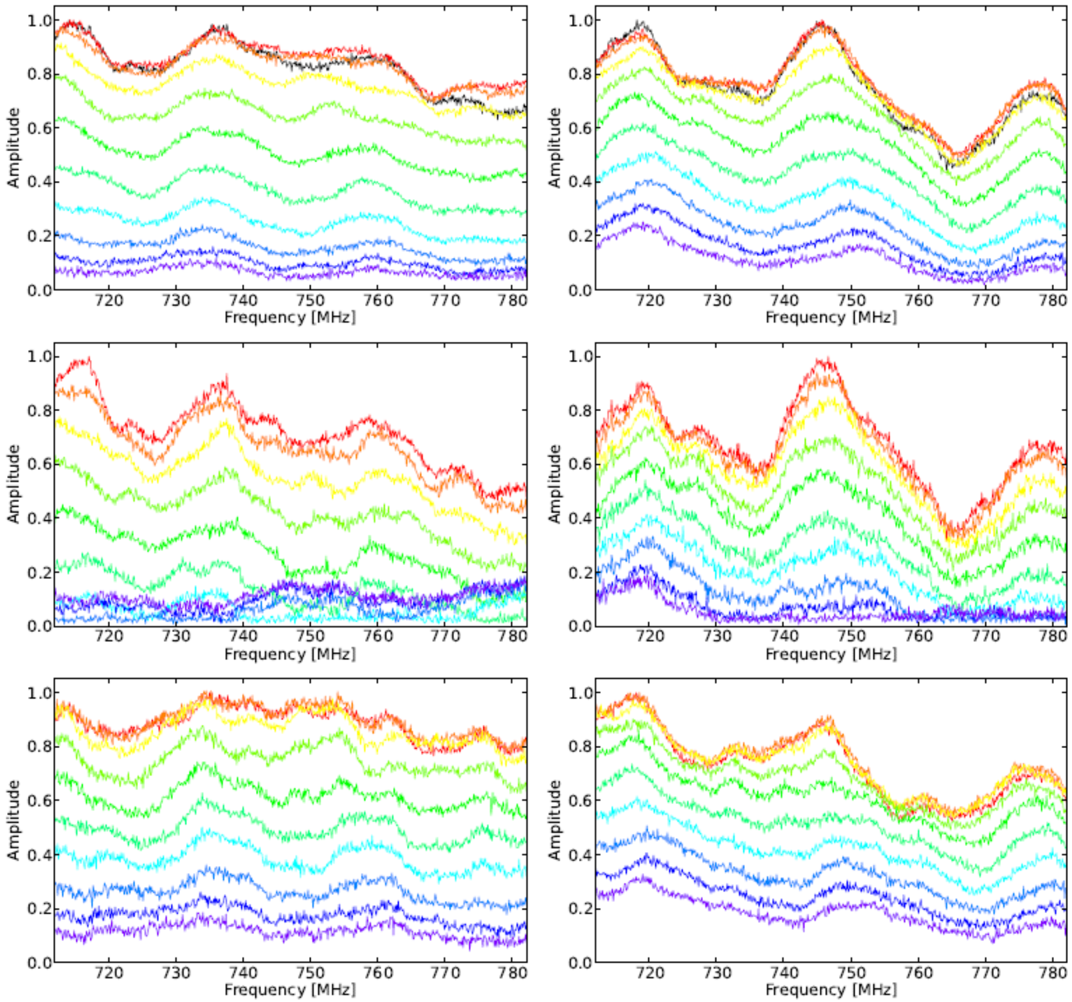

The transit process:
Purple → red

A4X-B9X	A4Y-B9Y
A4X-A4X	A4Y-A4Y
B9X-B9X	B9Y-B9Y

Cyg A flux (Perley, Butler, 2017)

$$\log S = \sum_{n=0}^{5} a_n [\log(\nu)]^n$$

5% difference in band.

- Transit process indicated from purple to red. $\Delta t = 1\ \mathrm{min}$
- Auto-correlation: background noise are removed.
- Black curves are square roots of auto-correlations.
  - Consistent to cross-correlation → Cyg A dominates the beam.

Calibration: bandpass comparison

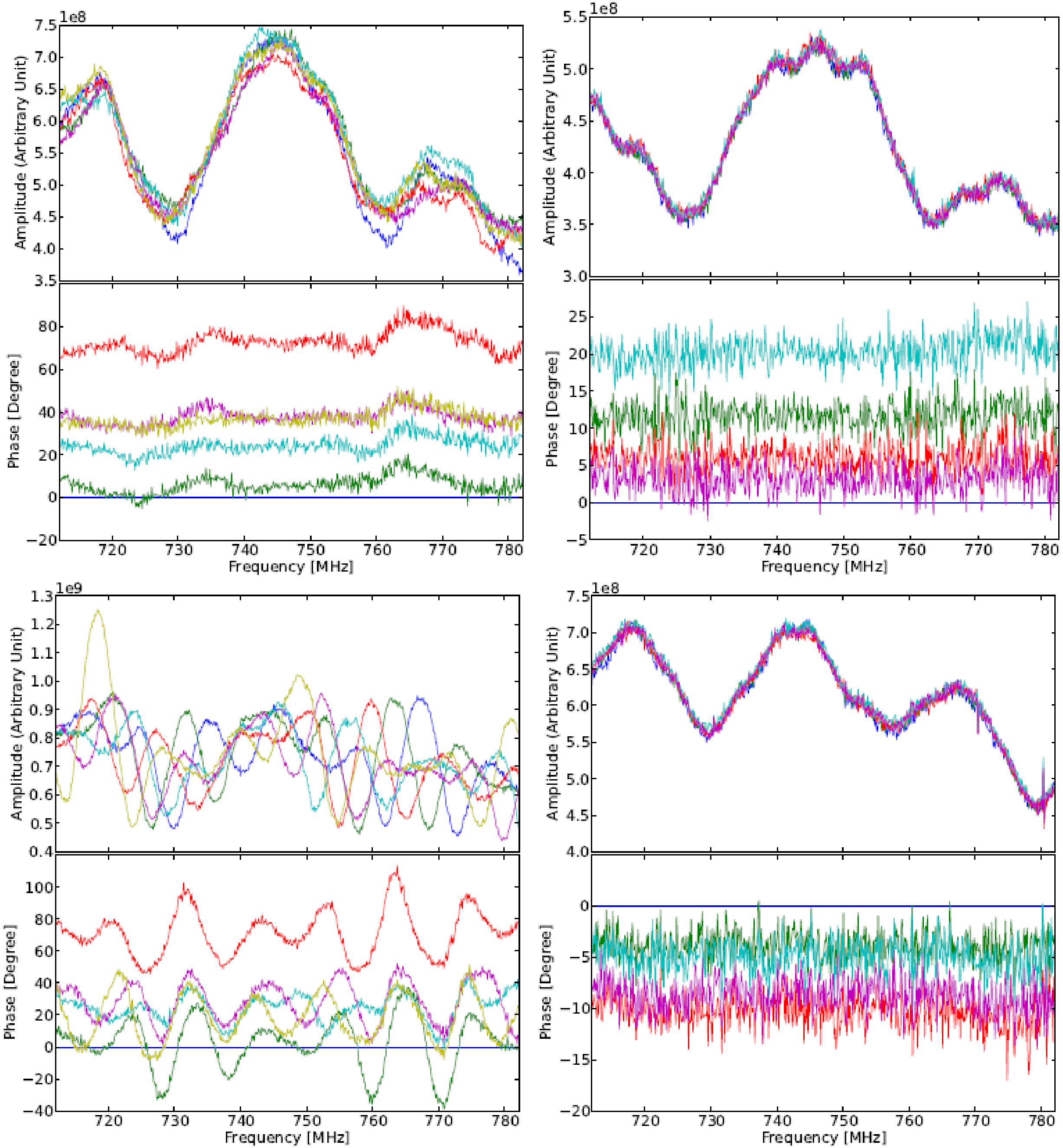

Left: 2018/03/22
Right: 2016/09/27

A2Y-B27Y	A2Y-B3Y
A13X-B31X	A6X-B13X

Phase @ Cyg A:

$$-\frac{2\pi\nu}{c}\vec{n}\cdot\overrightarrow{b_{ij}}+\varphi_{ij}(\nu)$$

- Amplitude and phase are stable among days.
- Sun in side lobe has a significant influence – Cyg A is not dominant any more.

Calibration: absolute calibration (Cyg A)

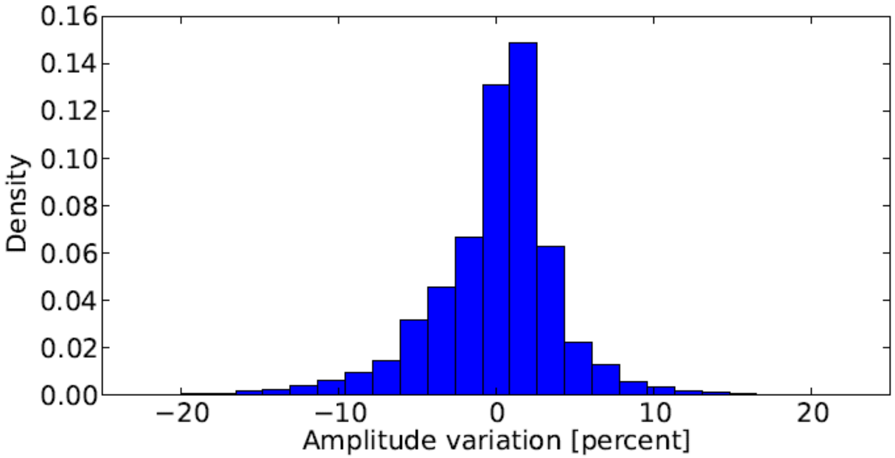

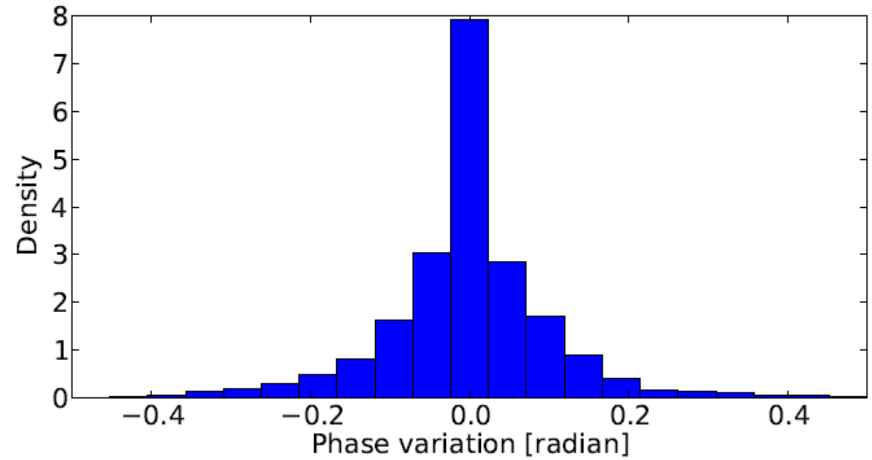

- Strong point source Cyg A:

$$V_{ij}^{0} = S_c \, G_i G_j^* \qquad G_i = g_i A_i(\hat{n}_0) e^{-i2\pi \hat{n}_0 \cdot \vec{u}_i}$$

- In matrix form:

$$\mathbf{V}_0 \;=\; S_c \mathbf{G}\mathbf{G}^{\dagger}$$

- Solve for $\mathbf{G}$ by solving for the eigenvectors of matrix $\mathbf{V} = \mathbf{V_0} + \mathbf{N}$ (Zuo et al. 2019)
- Condition:
  - Noise $\mathbf{N}$ is small compared to calibrator source.
- Gain variation in 5 days of 2016/09/27.

Calibration: relative calibration (CNS)

- Visibility of CNS (Calibrator Noise Source)
  - Not a point source $V_{ij}^{\rm CNS} \propto S_n e^{-i2\pi(\vec{n}_i \cdot \vec{r}_i - \vec{n}_j \cdot \vec{r}_j)}$
- Remove sky

$$V_{ij}^{\rm on} - V_{ij}^{\rm off} \approx C|G_{ij}|e^{-i2\pi\nu\Delta\tau_{ij}}e^{-i2\pi(r_i - r_j)/\lambda}$$

- Relative calibration tracks the instrumental phase variation.

- For feed channels
  - Fit baselines
  - $t \to 0, \Delta\varphi \to 0$
- Comparison

  Blue dots: relative calibration

  Green dots: absolute calibration

  Two calibration results

  are consistent @ Cyg A

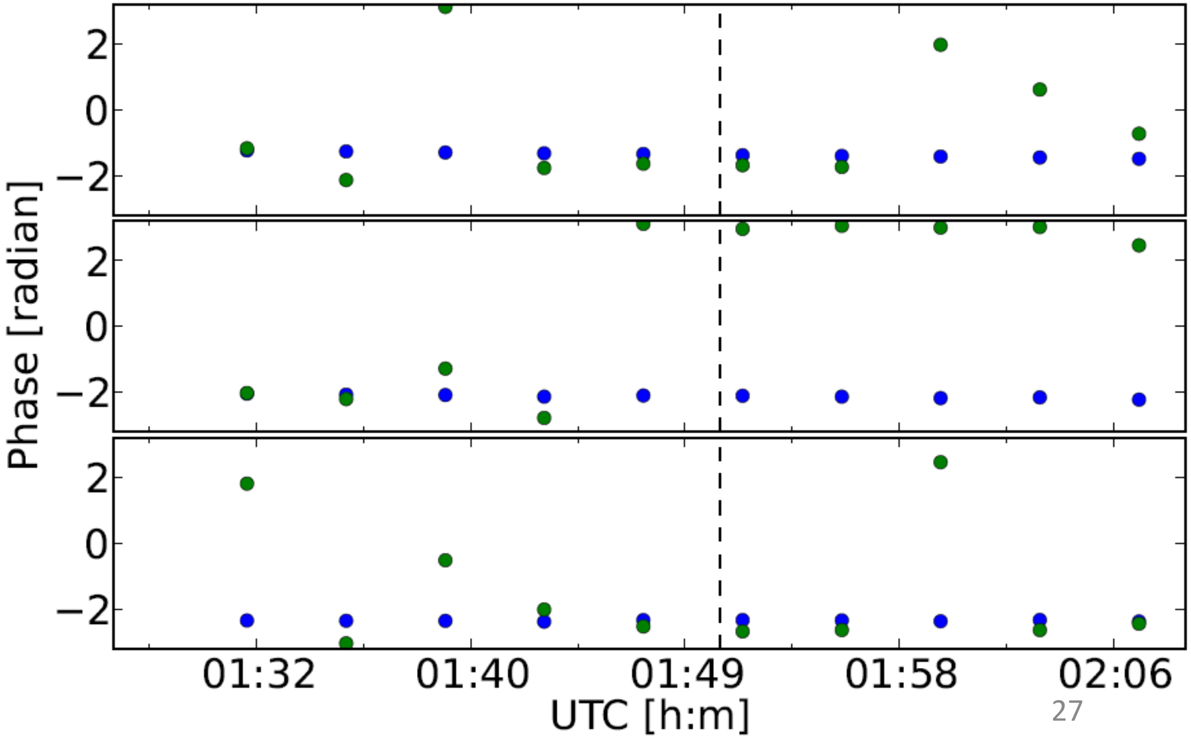

Calibration: relative calibration (CNS)

- Visibility of CNS (Calibrator Noise Source)
  - Not a point source $$V_{ij}^{\mathrm{CNS}} \propto S_n e^{-i2\pi(\vec{n}_i \cdot \vec{r}_i - \vec{n}_j \cdot \vec{r}_j)}$$
- Remove sky

$$V_{ij}^{\mathrm{on}} - V_{ij}^{\mathrm{off}} \approx C|G_{ij}|e^{-i2\pi\nu\Delta\tau_{ij}}e^{-i2\pi(r_i-r_j)/\lambda}$$

- Relative calibration tracks the instrumental phase variation.

- For feed pairs
  - $\Delta\varphi_{\mathrm{inst}} = \Delta\varphi_{\mathrm{CNS}}$
- Check by closure phase
  - The closure phase:

    $\phi_{ij} + \phi_{jk} + \phi_{ki} = 2N\pi$
- Baselines are calibrated individually.

- Deviations mostly $< 1^\circ$.
- Large deviations @ Sun

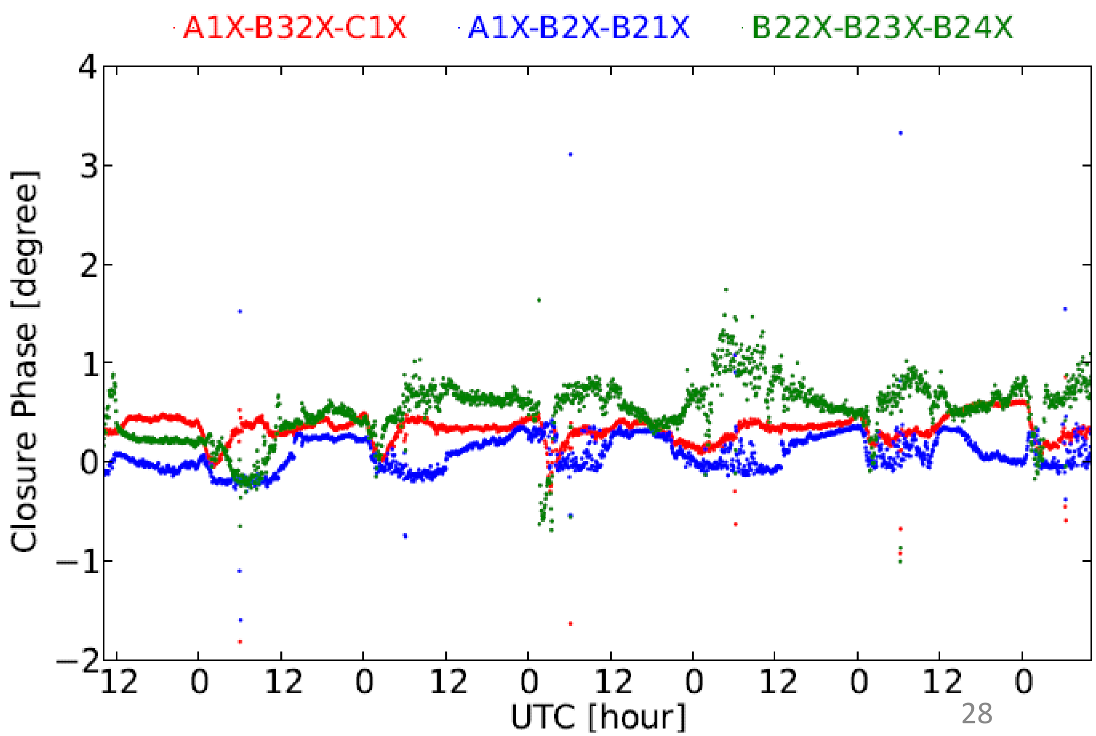

Calibration: stability of gain

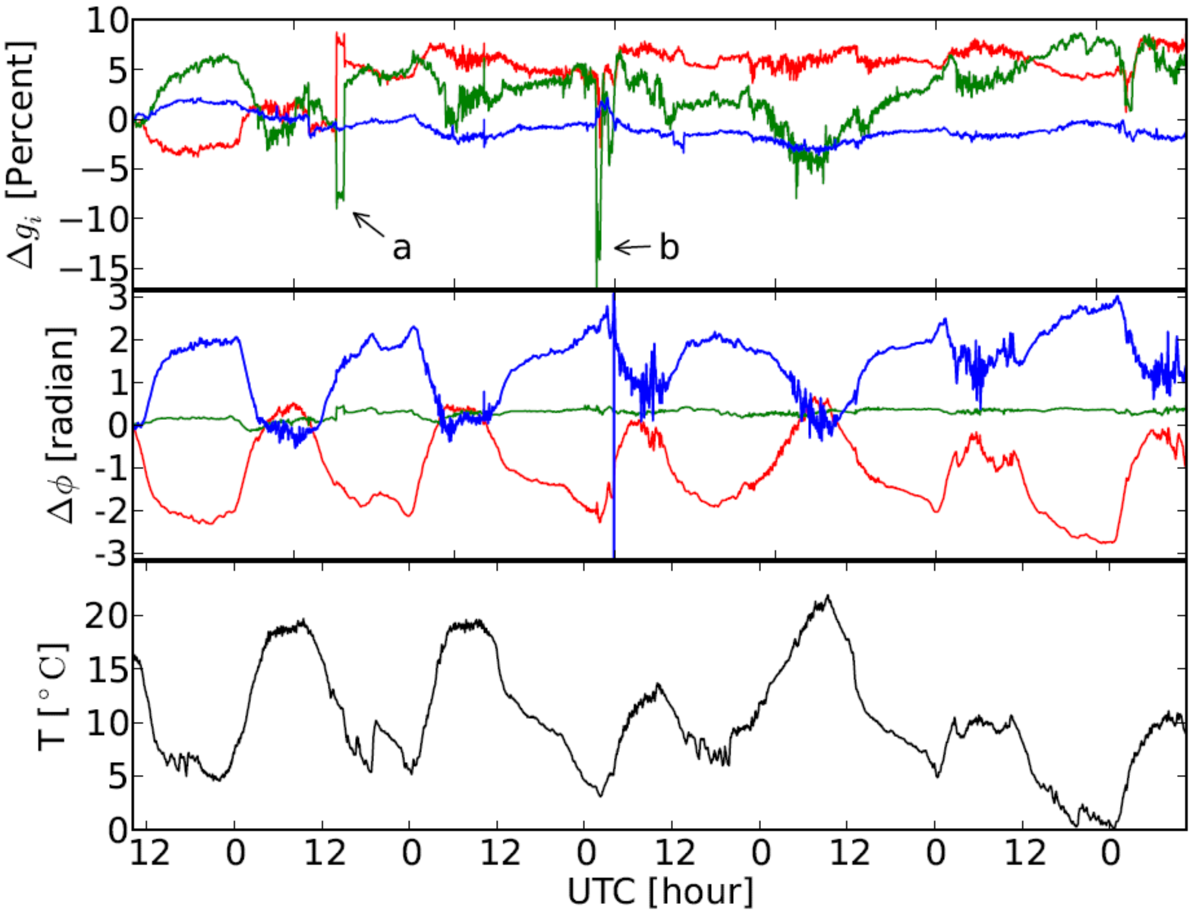

2018/03/22, 6 days' variation of gain.
Take 1st day as reference.

- Gain of single feed channel
- $\Delta\phi$ correlated with temperature
  - Optic cable result
- Gain:
  - Low at night
  - High in daytime
  - Larger variation in daytime.
- "a"
  - Dish pointing changed
- "b"
  - The rising Sun.
- Other variations
  - Rapid temperature change.
  - Big wind.
  - Unknown reasons.
- Amplitude may be inaccurate

System Temperature & SEFD

- Flux calibration by Cyg A
- Received power for single polarization channel

$$P_\nu = \frac{1}{2}\eta A_e f_{\mathrm{ps}} S_0$$

- Point source power $P_\nu = \eta k T_A^{\mathrm{ps}}$ (Antenna temperature T_A^{ps})
- For feed pair ab

$$V_{ab}^{\mathrm{ps}} = C T_A^{\mathrm{ps}}$$

- Method 1, auto-correlation
  - Receiver noise dominate

$$\bar{V}_{aa} = \langle n_a^* n_a \rangle = C\, T_{\mathrm{sys}}^{aa} \qquad T_{\mathrm{sys}}^{aa} = \frac{\bar{V}_{aa} T_A^{\mathrm{ps}}}{\Delta V_{aa}^{\mathrm{ps}}}$$

- Method 2, variation of auto-correlation

$$\sigma_{aa}^2 \equiv \langle |V_{aa} - \bar{V}_{aa}|^2 \rangle \quad \sigma_{aa} = C \frac{T_{\mathrm{sys}}^{aa}}{\sqrt{\delta\nu\delta t}} \qquad T_{\mathrm{sys}}^{aa} = \frac{\sigma_{aa}}{\Delta V_{aa}^{\mathrm{ps}}} T_A^{\mathrm{ps}} \sqrt{\delta\nu\delta t}$$

- Method 3, variation of cross-correlation

$$\sigma_{ab}^2 \equiv \langle |V_{ab} - \bar{V}_{ab}|^2 \rangle \quad \sigma_{ab} = C \frac{T_{\mathrm{sys}}^{ab}}{\sqrt{\delta\nu\delta t}} \qquad T_{\mathrm{sys}}^{ab} = \frac{\sigma_{ab}}{V_{ab}^{\mathrm{ps}}} T_A^{\mathrm{ps}} \sqrt{\delta\nu\delta t}$$

  - Transfer cross T_{sys}^{ab} to auto T_{sys}^{aa}
  - Same method in solving for pointing of cross-correlation.

System Temperature & SEFD

$$T_{\rm sys}^{aa} = \frac{\bar{V}_{aa} T_A^{\rm ps}}{\Delta V_{aa}^{\rm ps}} \qquad T_{\rm sys}^{aa} = \frac{\sigma_{aa}}{\Delta V_{aa}^{\rm ps}} T_A^{\rm ps} \sqrt{\delta\nu\delta t} \qquad T_{\rm sys}^{ab} = \frac{\sigma_{ab}}{V_{ab}^{\rm ps}} T_A^{\rm ps} \sqrt{\delta\nu\delta t}$$

- SEFD (System Equivalent Flux Density)

$$\mathrm{SEFD} \equiv \frac{2kT_{\rm sys}}{A_e} = \begin{cases} f_{\rm ps} S_0 \dfrac{\bar{V}_{aa}}{\Delta V_{aa}^{\rm ps}} \\ f_{\rm ps} S_0 \dfrac{\sigma_{aa}\sqrt{\delta\nu\delta t}}{V_{aa}^{\rm ps}} \\ f_{\rm ps} S_0 \dfrac{\sigma_{ab}\sqrt{\delta\nu\delta t}}{V_{ab}^{\rm ps}} \end{cases}$$

  - SEFD contains effective area: A_e

- From beam simulation, we have:

$$f_{\rm ps}^X = 0.9795,\ f_{\rm ps}^Y = 0.9908$$

$$A_e^X = 4.22\mathrm{m}^2,\ A_e^Y = 3.35\mathrm{m}^2$$

System Temperature & SEFD

$$T_{\rm sys}^{aa} = \frac{\bar{V}_{aa} T_A^{\rm ps}}{\Delta V_{aa}^{\rm ps}} \qquad T_{\rm sys}^{aa} = \frac{\sigma_{aa}}{\Delta V_{aa}^{\rm ps}} T_A^{\rm ps} \sqrt{\delta\nu\delta t} \qquad T_{\rm sys}^{ab} = \frac{\sigma_{ab}}{V_{ab}^{\rm ps}} T_A^{\rm ps} \sqrt{\delta\nu\delta t}$$

- SEFD

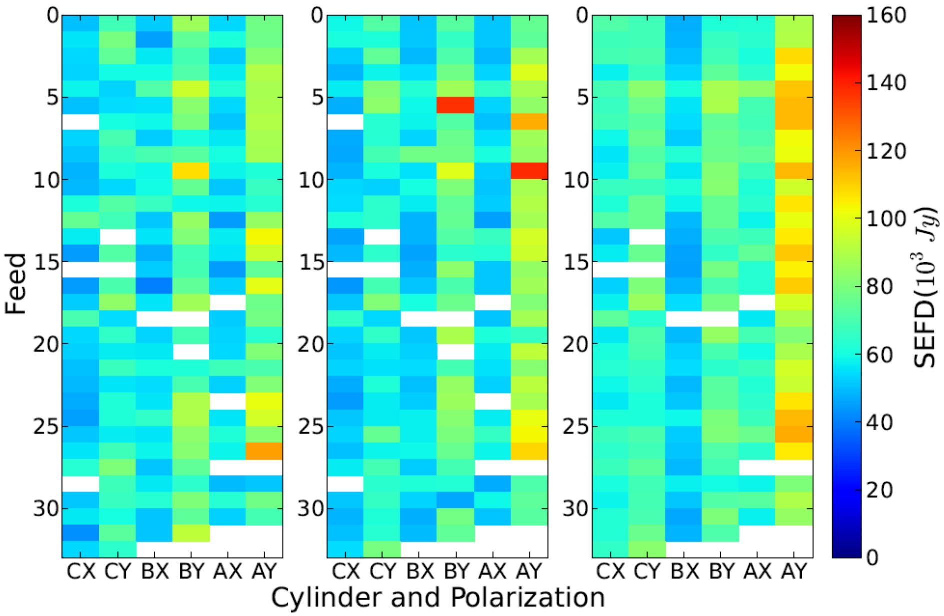

System temperature

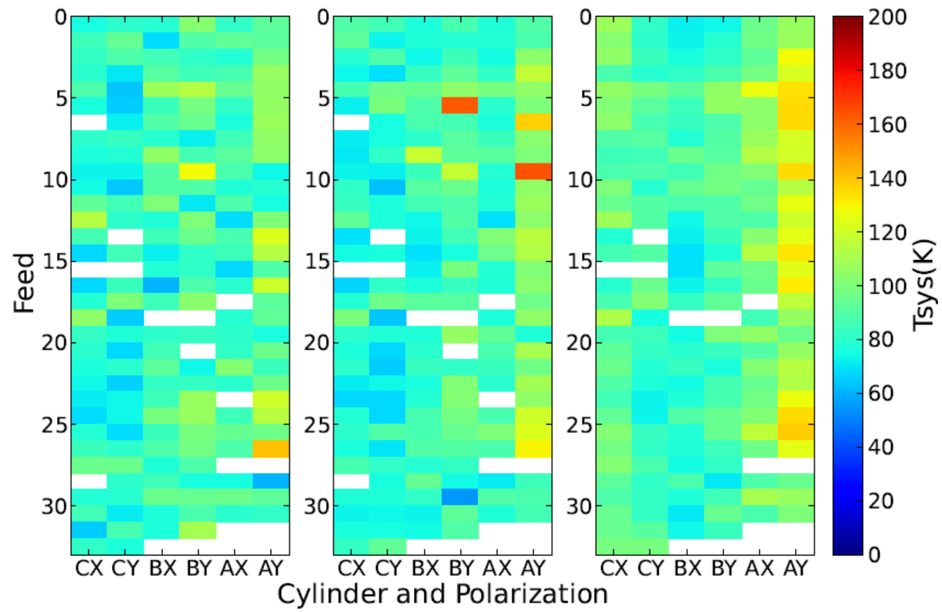

Pol	M1	M2	M3
X	55.1±6.4	53.9±5.83	60.1±7.92
Y	75.1±13.3	77.5±16.0	81.4±15.3

(Unit: 10^3 Jy)

Pol	M1	M2	M3	Mean
X	81.4	81.6	90.9	84.8
Y	91.0	91.7	96.7	93.3

(Unit: K)

Data analysis: integration time

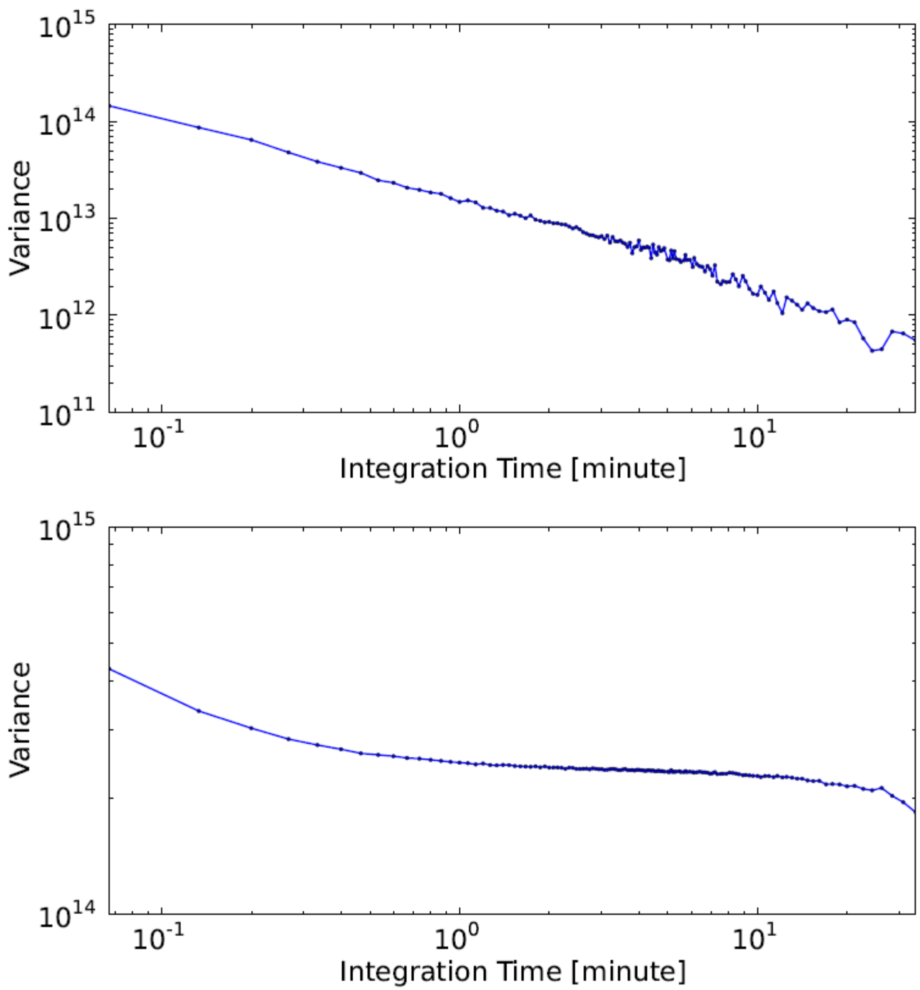

To observe HI, we should integrate data to suppress noise. How long?

Different cylinders:
A1Y-B2Y (2018/03/22 night)

Same cylinder:
A1Y-A2Y (2018/03/22 night)

- Short baselines hit ground ~ 1 minute.
- North-south baselines suffer heavy cross-coupling noises.
- Better to use long baselines spanning difference cylinders.

Reflections: stable wiggles

- Frequency response of individual device is flat.

- Stable sinusoidal wiggles in auto-correlation.
  - Wiggles are stable even in years.
  - Non-smooth structure makes foreground removal complex.

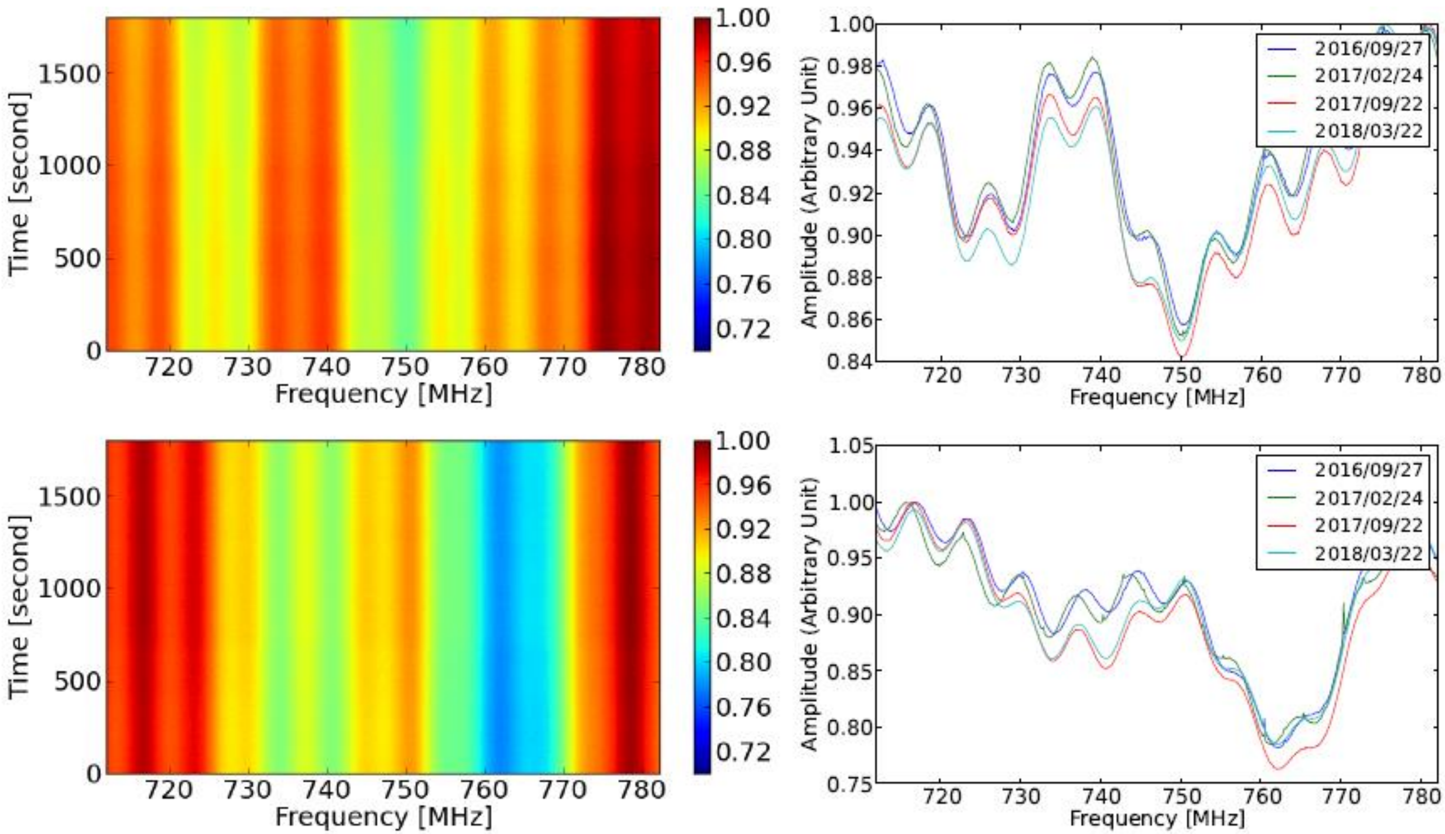

Top:
B22X-B22X

Bottom:
B22Y-B22Y

Reflections: model

- Reflections exist in signal chain.
  - Impedance mismatch.

- Voltage with reflection $\mathcal{E}'(\nu,t) = \mathcal{E}(\nu,t) + \epsilon(\nu)\mathcal{E}(\nu,t)$

- Reflection coefficient $\epsilon(\nu) = Ae^{i(2\pi\nu\tau+\phi)}$

- Visibility with reflection
$$\begin{aligned} V' &= [1 + (\epsilon + \epsilon^*) + \epsilon^*\epsilon)]\langle\mathcal{E}^*\mathcal{E}\rangle \\ &= [1 + 2A\cos(2\pi\nu\tau + \phi) + A^2]V \end{aligned}$$

- Multi-interfaces reflection

$$\mathcal{E}_i' = (1+\epsilon_i)\mathcal{E}_i \qquad \mathcal{E}'(\nu,t) = \mathcal{E}(\nu,t)\prod_j[1+\epsilon_j(\nu)]$$

$$V' = V\prod_i[1 + 2A_i\cos(2\pi\nu\tau_i + \phi_i) + A_i^2]$$

Reflections: delay transform

- Fourier transforming the auto-correlation spectrum into delay spectrum:

$$\tilde{V}(\tau) = \int W(\nu)V(\nu)e^{i2\pi\nu\tau}\mathrm{d}\nu$$

- In discrete form (Hann window to decrease spectrum leakage):

$$\tilde{V}(\tau) = \sum_n W_n V(\nu_n)e^{i2\pi\nu_n\tau} \qquad W(n) = 0.5 - 0.5\cos\left(\frac{2\pi n}{M-1}\right), \qquad (0 \leq n \leq (M-1))$$

- Increase resolution from 576 points to 16384 points.

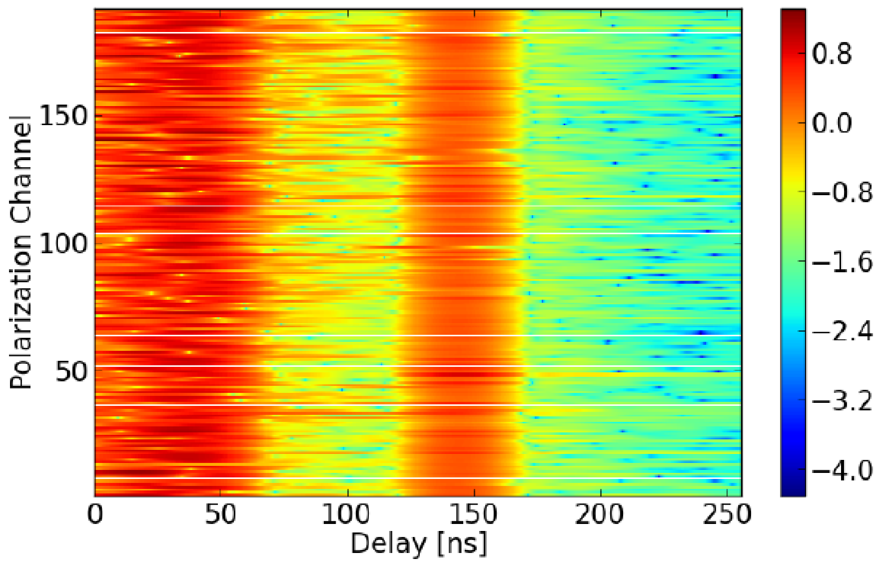

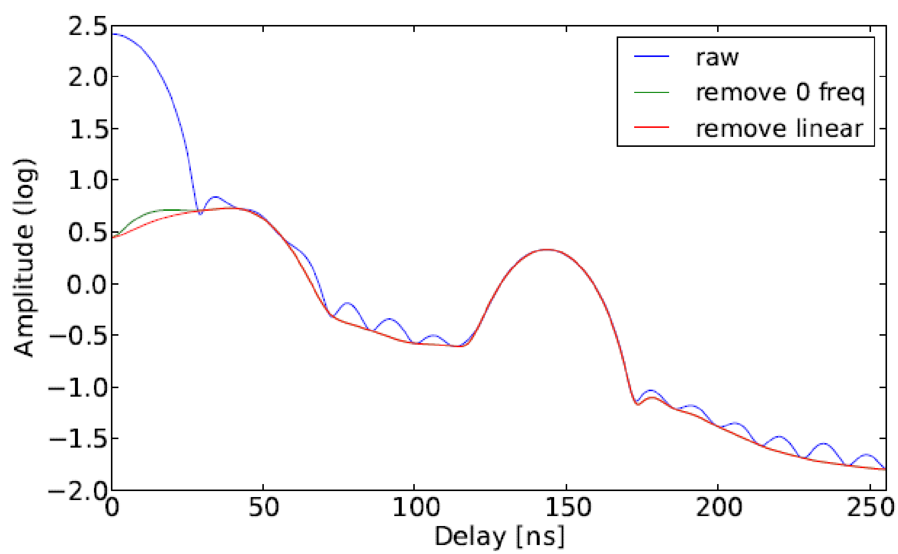

Two peaks @ ~ 142 ns and $0 \sim 60$ ns

Reflections: origin

- Time delay $\tau = \frac{2L}{v}$, where $v = \frac{c}{\sqrt{\varepsilon_r \mu_r}}$
  - For most coaxial cables, $v \approx 0.7c$ (Pozar, 2009).

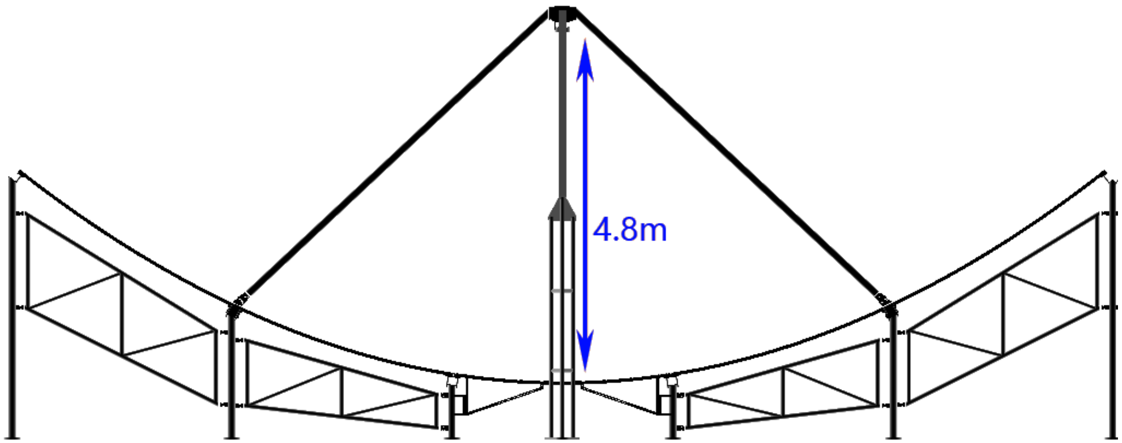

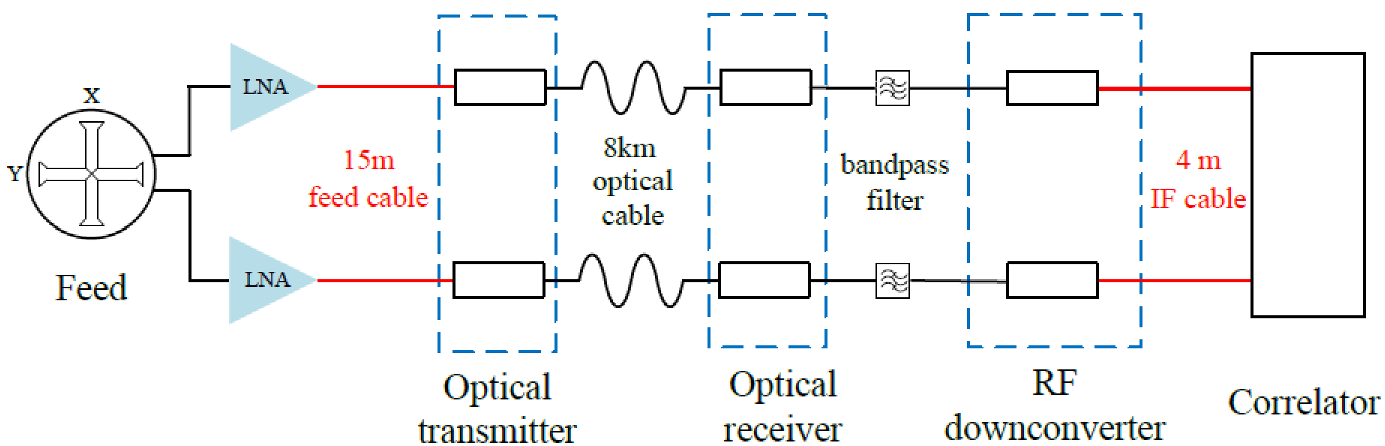

Reflections: antenna simulation

- Simulation of 1 feed plus antenna.
- Directivity of center beam at different frequencies.

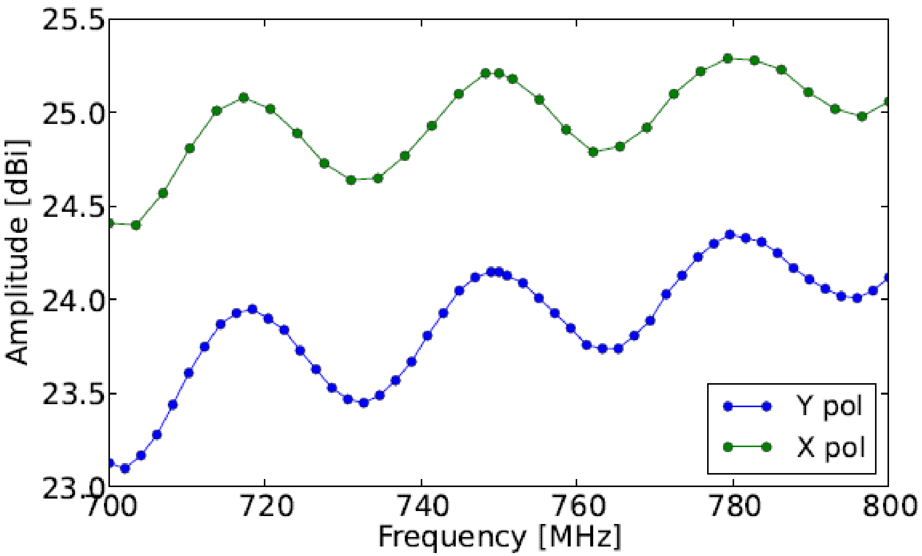

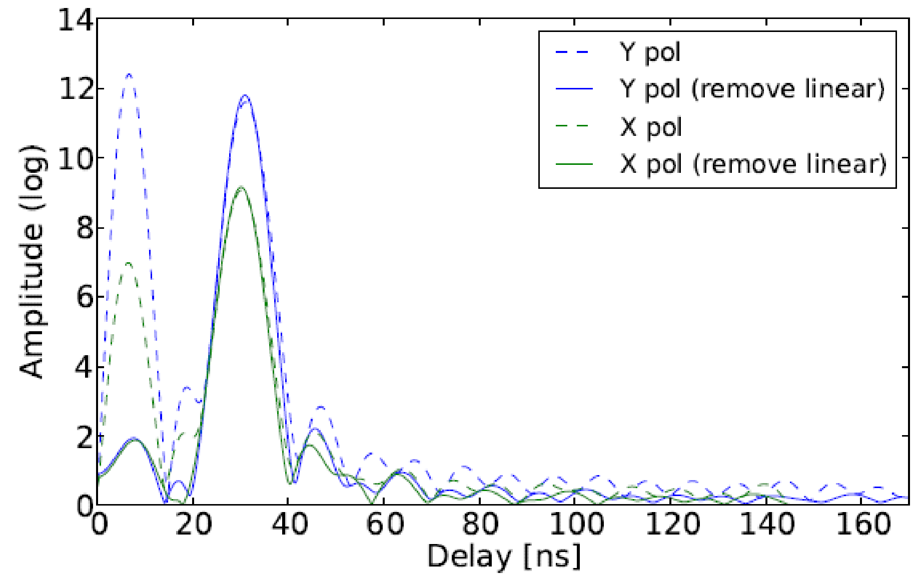

- Part of <60ns peak is confirmed to be caused by standing waves between antenna reflector and feed (peak ~31ns)

- Also consider IF cable part.

Reflections: experiment verification

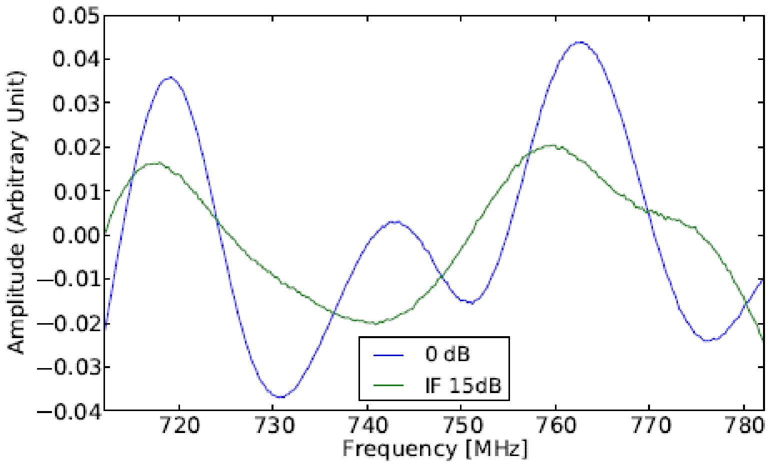

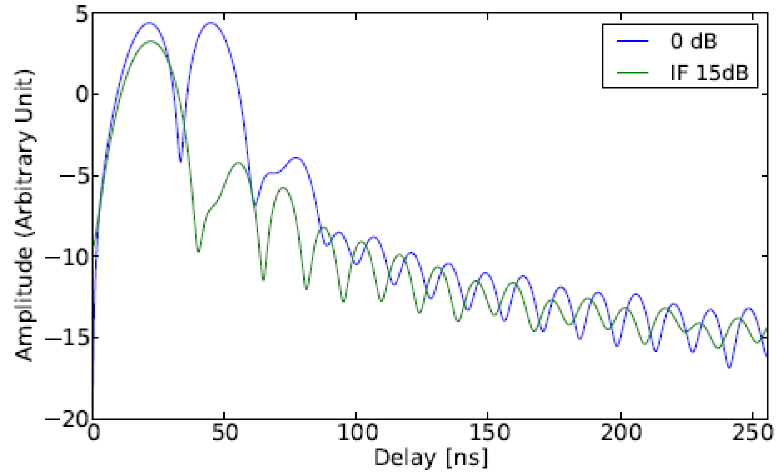

- Insert 15 dB attenuator in IF cable. (Flat noise as mixer input.)
- Part of <60ns peak is confirmed to be caused by IF cable (peak of $\sim 42\text{ns}$).
- Other peak needs further analysis.

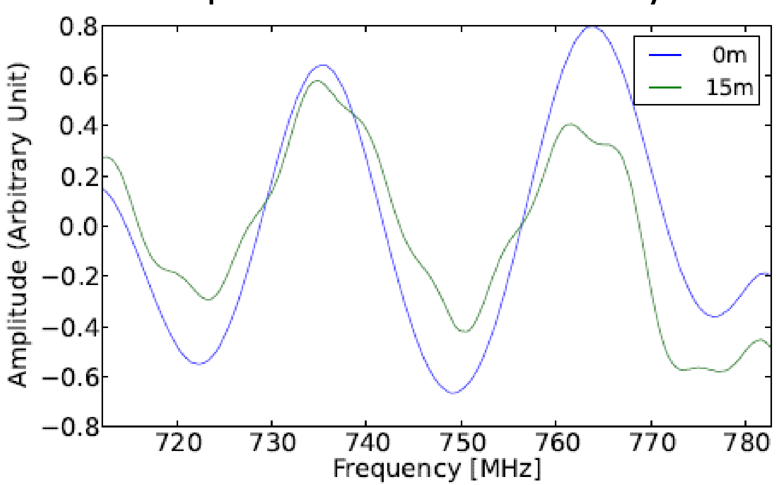

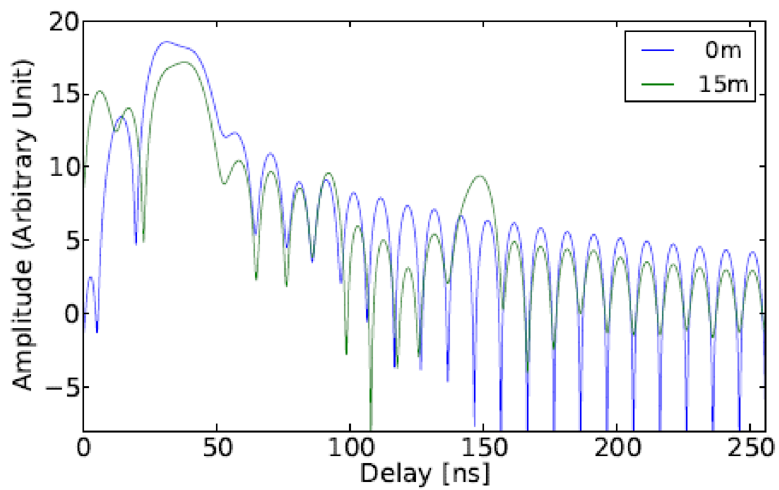

- Insert 15-meter cable after LNA.
- $\sim 142\text{ns}$ peak is confirmed to be caused by 15-meter feed cable.

Reflections: different sources

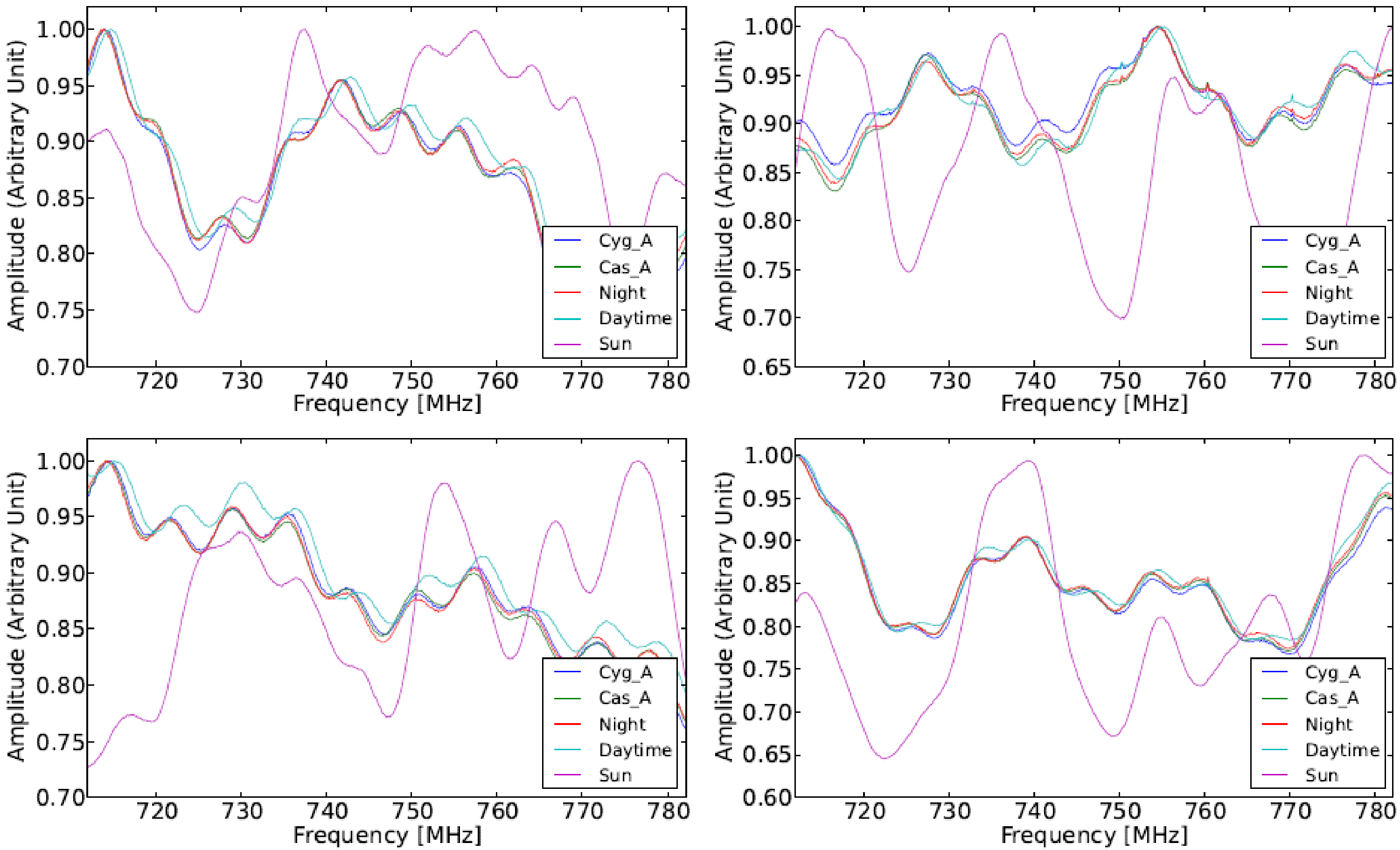

A1Y	B15Y
A3X	A23X

Averaged over 40 seconds

- Compare Cyg A, Cas A, night data, daytime data, Sun's data.
- Reflections are similar @ different sources, except the Sun.

Reflections: delay spectra of different sources

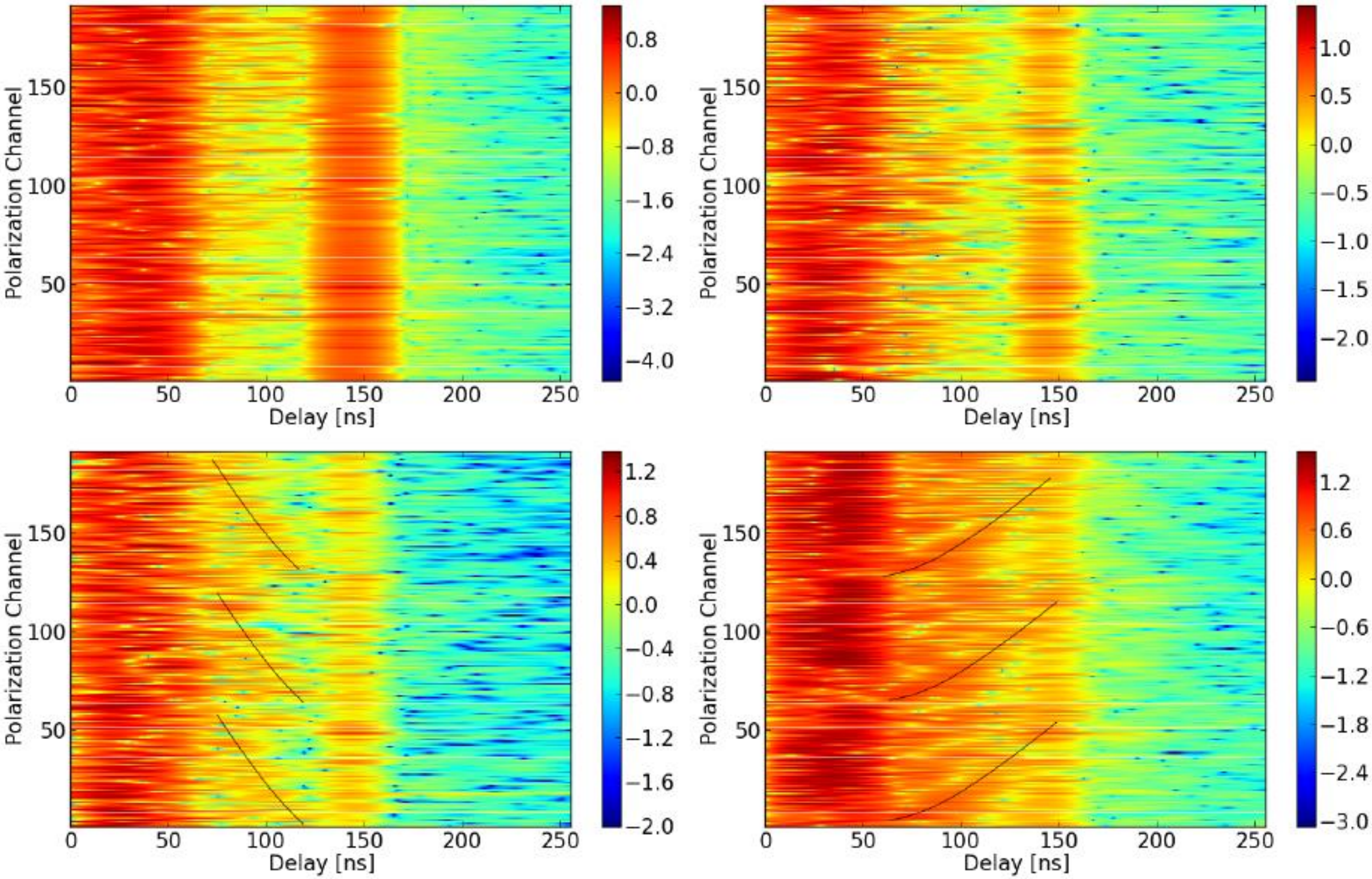

Night	Cyg A
Cas A	Sun

- Delay spectra of all polarization channels.
- Similar patterns are found across all channels.
- Feather-like features are related to sources’ zenith angles.
- Reflections are related to source’s zenith angle → calibration difficulty.

Reflections: mean delay spectra of different sources

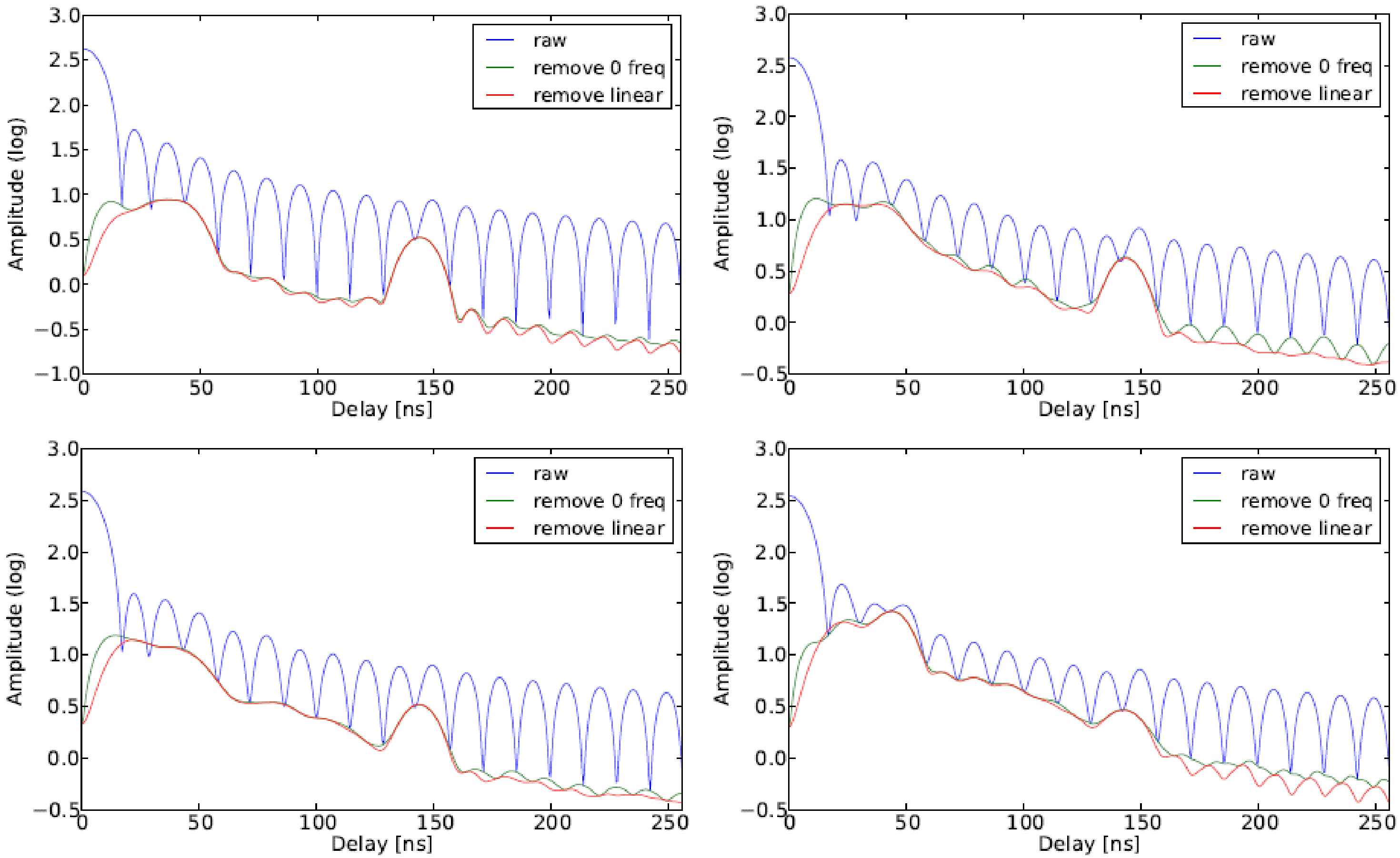

Night	Cyg A
Cas A	Sun

- Averaged delay spectra of all polarization channels.
- Similar delay peaks are found.
- For Sun, ~ 142 ns is weak.
  - Scatter source reflection effects counteracted.
  - Normalization.

Reflections: reflection calibration

- 1. In delay spectrum, make initial estimate
  - $\tau_0 = \tau_{\text{peak}}, A_0 = \frac{|\tilde{V}(\tau=\tau_{\text{peak}})|}{|\tilde{V}(\tau=0)|}$
- 2. reflection correction
  - $V^{\text{cal}} = V(1+\varepsilon)(1+\varepsilon^*)$, where $\varepsilon = Ae^{i(2\pi\nu\tau+\phi)}$
- 3. minimize and iterate over other peaks.

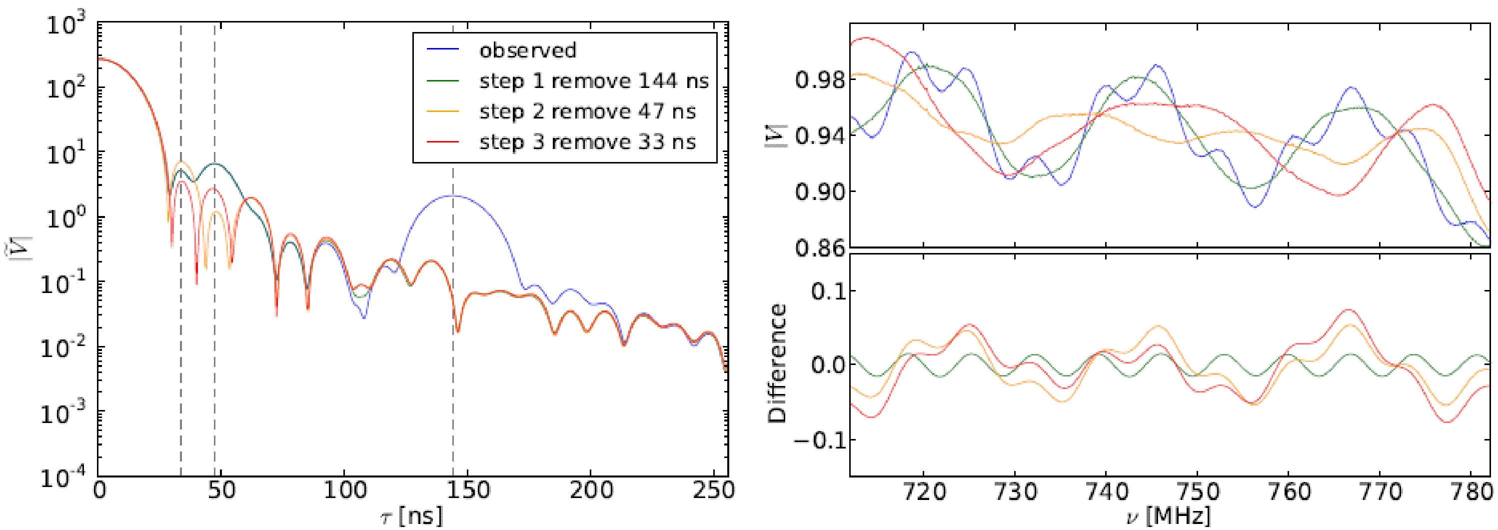

Next work:
Mitigate/remove reflections by hardware improvement.

Peak	A	τ(ns)	ϕ(rad)
1	7.80×10^{-3}	144.6	7.19
2	2.12×10^{-2}	45.6	0.31
3	1.37×10^{-2}	31.0	8.30

Summary

- Tianlai system and observation
- Tianlai cylinder performance analysis
  - Hardware performance experiments
    - Gain, linearity, bandpass, pointing
    - Antenna LNA, optic cable, feed, mixer, correlator
  - Absolute calibration (Cyg A) and relative calibration (CNS)
  - System temperature ($\sim 90\mathrm{K}$) and SEFD
- Reflections in the Tianlai system
  - ~ 142 ns → 15-m feed cable
  - $0 \sim 60$ ns → standing waves in antenna, 4-m IF cable, other.
  - Reflection is related to source's zenith angle.
  - Reflection removal.
- See papers for detail:
  - https://link.springer.com/article/10.1007/s11433-020-1594-8
  - http://www.raa-journal.org/docs/papers_accepted/2020-0198.pdf
  - https://arxiv.org/abs/2011.10757

Thanks!